SUPPLEMENTARY MATERIAL:

An 8-hydroxyquinoline-proline hybrid with multidrug resistance reversal activity and solution chemistry of its half-sandwich organometallic Ru and Rh complexes

János P. Mészáros,[a,b] Jelena M. Poljarevic,[a,c] István Szatmári,[d] Oszkár Csuvik,[d] Ferenc Fülöp,[d] Norbert Szoboszlai,[e] Gabriella Spengler,[b,f] Éva A. Enyedy[a,b]*

[a] Department of Inorganic and Analytical Chemistry, Interdisciplinary Excellence Centre, University of Szeged, Dóm tér 7, H-6720 Szeged, Hungary

[b] MTA-SZTE Lendület Functional Metal Complexes Research Group, University of Szeged, Dóm tér 7, H-6720 Szeged, Hungary

[c] Faculty of Chemistry, University of Belgrade, Studentski trg. 12-16, 11000 Belgrade, Serbia

[d] Institute of Pharmaceutical Chemistry and Stereochemistry Research Group of Hungarian Academy of Sciences, University of Szeged, Eötvös u. 6, H-6720 Szeged, Hungary

[e] Laboratory for Environmental Chemistry and Bioanalytics, Institute of Chemistry, Eötvös Lóránd University, Pázmány Péter stny. 1/A, H-1117 Budapest, Hungary

[f] Department of Medical Microbiology and Immunobiology, University of Szeged, Dóm tér 10, H-6720 Szeged, Hungary

1.

HQCl-Pro

^{1}H NMR (CD_3OD, ppm): δ 8.945 (dd, J = 4.19 Hz, ^{4}J = 1.49 Hz, 1H, H(2)), δ 8.573 (dd, J = 8.56 Hz, ^{4}J = 1.51 Hz, 1H, H(4)), δ 7.736 (s, 1H, H(6)), δ 7.703 (dd, J = 8.57 Hz, 4.19 Hz, 1H, H(3)), δ 4.657 (d, J = 13.00 Hz, 1H, H(9)), δ 4.511 (d, J = 13.00 Hz, 1H, H(9)), δ 4.044 (dd, J = 9.34 Hz, 5.79 Hz, 1H, H(11)), δ 3.618 (m, 1H, H(14)), δ 3.298 (m, 1H, (H14, under solvent peak)), δ 2.474 (m, 1H, H(12)), δ 2.181 (m, 1H, H(12)), δ 2.117 (m, 1H, H(13)), δ 1.946 (m, 1H, H(13)).

^{13}C NMR (CD_3OD, ppm): δ 173.34 (C(15)), δ 153.62 (C(8)), δ 150.79 (C(2)), δ 140.29 (C(8a)), δ 134.04 (C(4)), δ 130.16 (C(6)), δ 128.45 (C(5)), δ 124.75 (C(3)), δ 121.56 (C(4a)), δ 114.51 (C(7)), δ 70.39 (C(11)), δ 55.59 (C(14)), δ 54.23 (C(9)), δ 30.06 (C(12)), δ 24.42 (C(13)).

[Ru(η^6-*p*-cym)(L)Cl]

^{1}H NMR (CD_3OD, ppm): δ 9.360 (t, J = 4.19 Hz, 1H, H_{lig}(2)), δ 8.517 (d, J = 8.63 Hz, 1H, H_{lig}(4)), δ 7.722 (m, 1H, H_{lig}(3)), δ 7.519 (s, 0.34 H, H_{lig}(6)), δ 7.450 (s, 0.66H, H_{lig}(6)), δ 5.875 (m, 2H, H_{cym}(C3)), δ 5.632 (m, 2H, H_{cym}(C2)), δ 4.851 (d, J = 13.21 Hz, 0.66 H, H_{lig}(9)), δ 4.651 (m, 1H, H_{lig}(9)), δ 4.519 (d, J = 12.96 Hz, 0.34H, H_{lig}(9)), δ 4.394 (dd, J = 9.37 Hz, 5.79 Hz, 0.66H, H(11)), δ 4.296 (d, J = 13.3 Hz, 0.66H, H_{lig}(9)), δ 3.538 (m, 1H, H_{lig}(14)), δ 3.053 (q, J = 8.9 Hz, 0.66H, H_{lig}(14)), δ 2.858 (m, 0.66H, H_{cym}(C5)), δ 2.809 (m, 0.34H, H_{cym}(C5)), δ 2.565 (m, 1H, H_{lig}(12)), δ 2.303 (m, 1H, H_{lig}(12)), δ 2.263 (s, 2H, H_{cym}(C7)), δ 2.253 (s, 1H, H_{cym}(C7)), δ 2.111 (m, 1H, H_{lig}(13)), δ 1.948 (m, 1H, H_{lig}(13)), δ 1.194 (m, 6H, J = 7.5 Hz, H_{cym}(C6)).

^{13}C NMR (CD_3OD, ppm): δ 171.87 (C(15)), δ 168.69 and 167.64 (C(8)), δ 153.01 and 152.84 (C(2)), δ 145.95 and 145.29 (C(8a)), δ 135.84 and 135.78 (C(4)), δ 132.09 and 130.61 (C(6)), δ 129.69 and 129.28 (C(5)), δ 125.61 and 125.47 (C(3)), δ 115.95 and 115.22 (C(4a)), δ 114.36 and 113.99 (C(7)), δ 103.42 and 103.19 (C(C4)), δ 100.27 and 99.82 (C(C1)), δ 84.10, 83.91, 83.45, 83.43, 82.91, 82.61, 82.16 and 81.93 (C(C3 and C2)), δ 68.44 (C(11)), δ 57.18 and 54.81 (C(14)), δ 55.34 and 54.54 (C(9)), δ 32.30 and 32.24 (C(C5)), δ 30.02 and 29.13 (C(12)), δ 24.20 and 23.63 (C(13)), δ 22.52, 22.50, 22.35 and 22.30 (C(C6)), δ 18.76 and 18.69 (C(C7)).

[Ru(η^6-tol)(L)Cl]

^{1}H NMR (CD_3OD, ppm): δ 9.403 (t, J = 3.81 Hz, 1H, H_{lig}(2)), δ 8.512 ((d, J = 8.53 Hz, ^{4}J = 3.27 Hz, 1H, H_{lig}(4)), δ 7.713 (m, 1H, H_{lig}(3)), δ 7.521 (s, 0.34 H, H_{lig}(6)), δ 7.458 (s, 0.66H, H_{lig}(6)), δ 6.016 (m, 2H, H_{tol}(T3)), δ 5.615 (m, 3H, H_{tol}(T2 and T4)), δ 4.836 (d, J = 13.15 Hz, 0.66 H, H_{lig}(9)), δ 4.670 (d, J = 13.36 Hz, 0.34H, H_{lig}(9)), δ 4.518 (d, J = 12.96 Hz, 0.34H, H_{lig}(9)), δ 4.380 (dd, J = 9.19 Hz, 5.66 Hz, 0.66H, H(11)), δ 4.327 (d, J = 13.14 Hz, 0.66H, H_{lig}(9)), δ 3.567 (m, 1H, H_{lig}(14)), δ 3.090 (q, J = 8.5 Hz, 0.66H, H_{lig}(14)), δ 2.550 (m, 1H, H_{lig}(12)), δ 2.326 (s, 2H, H_{tol}(T5)), δ 2.308 (s, 1H, H_{tol}(T5)), δ 2.118 (m, 1.5H, H_{lig}(12 and 13)), δ 1.946 (m, 1H, H_{lig}(13)).

^{13}C NMR (CD_3OD, ppm): δ 171.93 and 171.83 (C(15)), δ 168.83 and 167.80 (C(8)), δ 153.24 and 153.06 (C(2)), δ 146.20 and 145.50 (C(8a)), δ 135.83 and 135.76 (C(4)), δ 132.22 and 130.71 (C(6)), δ 129.75 and 129.36 (C(5)), δ 125.58 and 125.44 (C(3)), δ 115.94 and 115.12 (C(4a)), δ 114.37 and 114.01 (C(7)), δ 102.89 and 102.85 (C(T1)), δ 89.07, 89.02, 87.11 and 87.07 (C(T3)), δ 81.24, 81.09, 80.92 and 80.87 (C(T2)), δ 79.04 and 78.91 (C(T4)), δ 68.42 and 67.78 (C(11)), δ 57.18 and 54.96 (C(14)), δ 55.47 and 54.21 (C(9)), δ 29.97 and 29.21 (C(12)), δ 24.18 and 23.66 (C(13)), δ 19.05 and 19.03 (C(T5)).

[Rh(η^5-C_5Me_5)(L)Cl]

^{1}H NMR (CD_3OD, ppm) δ 8.945 (d, J = 4.9 Hz, 1H, H_{lig}(2)), δ 8.558 (d, J = 9.3 Hz, 1H, H_{lig}(4)), δ 7.773 (dd, J = 9.2 Hz, 5.1 Hz, 1H, H_{lig}(3)), δ 7.550 (s, 0.34H, H_{lig}(6)), δ 7.481 (s, 0.66H, H_{lig}(6)), δ 4.944 (d, J = 9.3 Hz, 0.66H, H_{lig}(9)), δ 4.678 (d, J = 9.3 Hz, 0.34H, H_{lig}(9)), δ 4.516 (d, J = 9.3 Hz, 0.34H, H_{lig}(9)), δ 4.399 (t, J = 9.3 Hz, 0.66H, H_{lig}(11)), δ 4.211 (d, J = 9.3 Hz, 0.66H, H_{lig}(9)), δ 3.558 (m, 1H, H_{lig}(14)), δ 3.065 (q, J = 9.3 Hz, 1H, H_{lig}(14)), δ 2.577 (m, 1H, H_{lig}(12)), δ 2.291 (m, 0.66H, H_{lig}(12)), δ 2.114 (m, 1.5H, H_{lig}(13)), δ 2.114 (m, 1.5H, H_{lig}(13)), δ 1.953 (m, 1H, H_{lig}(13)), δ 1.776 (s, 15H, H_{C5Me5}(CH_3)).

^{13}C NMR (CD_3OD, ppm): δ 171.66 (C(15)), δ 166.76 (C(8)), δ 150.14 and 150.04 (C(2)), δ 145.95 (C(8a)), δ 136.06 (C(4)), δ 132.78 and 131.16 (C(6)), δ 129.76 (C(5)), δ 125.78 and 125.64 (C(3)), δ 116.00 (C(4a)), δ 113.82 (C(7)), δ 95.96 (C(C_5)), δ δ 68.74 (C(11)), δ 57.54 (C(14)), δ 55.14 and 54.50 (C(9)), δ 29.93 and 29.27 (C(12)), δ 24.00 (C(13)), δ 8.97 (C(Me_5)).

2.

pH-potentiometry: The exact concentration of the ligand stock solutions together with the proton dissociation constants were determined by pH-potentiometric titrations with the use of the computer program Hyperquad2013.[1] The aqueous [Rh(η^5-C_5Me_5)(H_2O)$_3$](NO_3)$_2$, [Ru(η^6-*p*-cym)(H_2O)$_3$](NO_3)$_2$ and [Ru(η^6-tol)(H_2O)$_3$](NO_3)$_2$ stock solutions were obtained by dissolving an exact amount of the dimeric precursor in water followed by addition of equivalent amounts of $AgNO_3$ to remove chloride ions. The exact concentrations of chloride ion containing and chloride-free metal ion stock solutions were determined by pH-potentiometric titrations employing stability constants for [(Rh(η^5-C_5Me_5))$_2$(μ-OH)$_i$]$^{(4-i)+}$, [(Ru(η^6-tol))$_2$(μ-OH)$_i$]$^{(4-i)+}$ and [(Ru(η^6-*p*-cym))$_2$(μ-OH)$_i$]$^{(4-i)+}$ (i = 2 or 3) complexes.[2,3]

Determining proton dissociation constants of ligands and stability constants for the metal complexes were carried out at 25.0 ± 0.1 °C in water in the pH range between 2.0 and 11.5, and at a constant ionic strength of 0.20 M KNO_3. The titrations were performed in a carbonate-free KOH solution (0.20 M). The exact concentrations of HNO_3 and KOH solutions were determined by pH-potentiometric titrations. An Orion 710A pH-meter equipped with a Metrohm combined electrode (type 6.0234.100) and a Metrohm 665 Dosimat burette were used for the pH-potentiometric measurements. The electrode system was calibrated according to the method suggested by Irving *et al*.[4] The average water ionization constant, pK_w, was determined as 13.76 ± 0.01, which is in good agreement with literature data.[5] The initial volume of the samples was 5.0 mL. The ligand concentration was 2.0 mM. Samples

were degassed by bubbling purified argon through them for about 10 minutes prior to the measurements and the inert gas was also passed over the solutions during the titrations.

3.

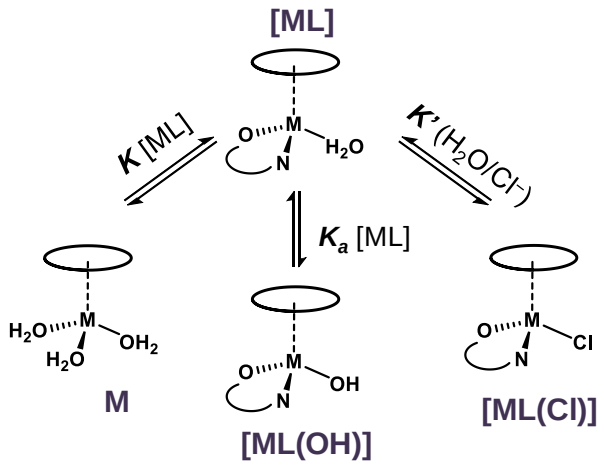

Scheme S1. Processes in the $[M(\eta^{6/5}\text{-arene/arenyl})(H_2O)_3]^{2+}$ – HQCl-Pro systems

4.

Figs. S1-S12. CHARACTERIZATION OF LIGAND AND COMPLEXES:

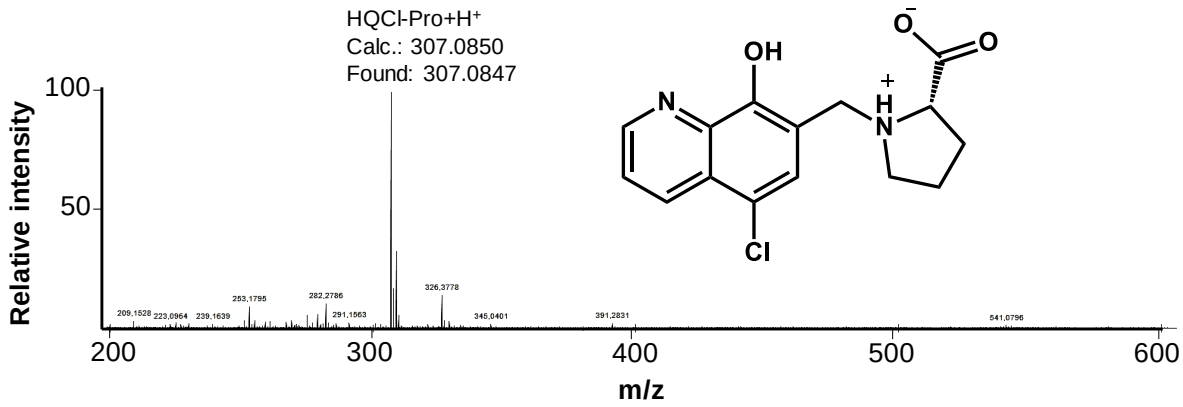

Fig. S1. ESI-MS spectrum of HQCl-Pro in positive mode.

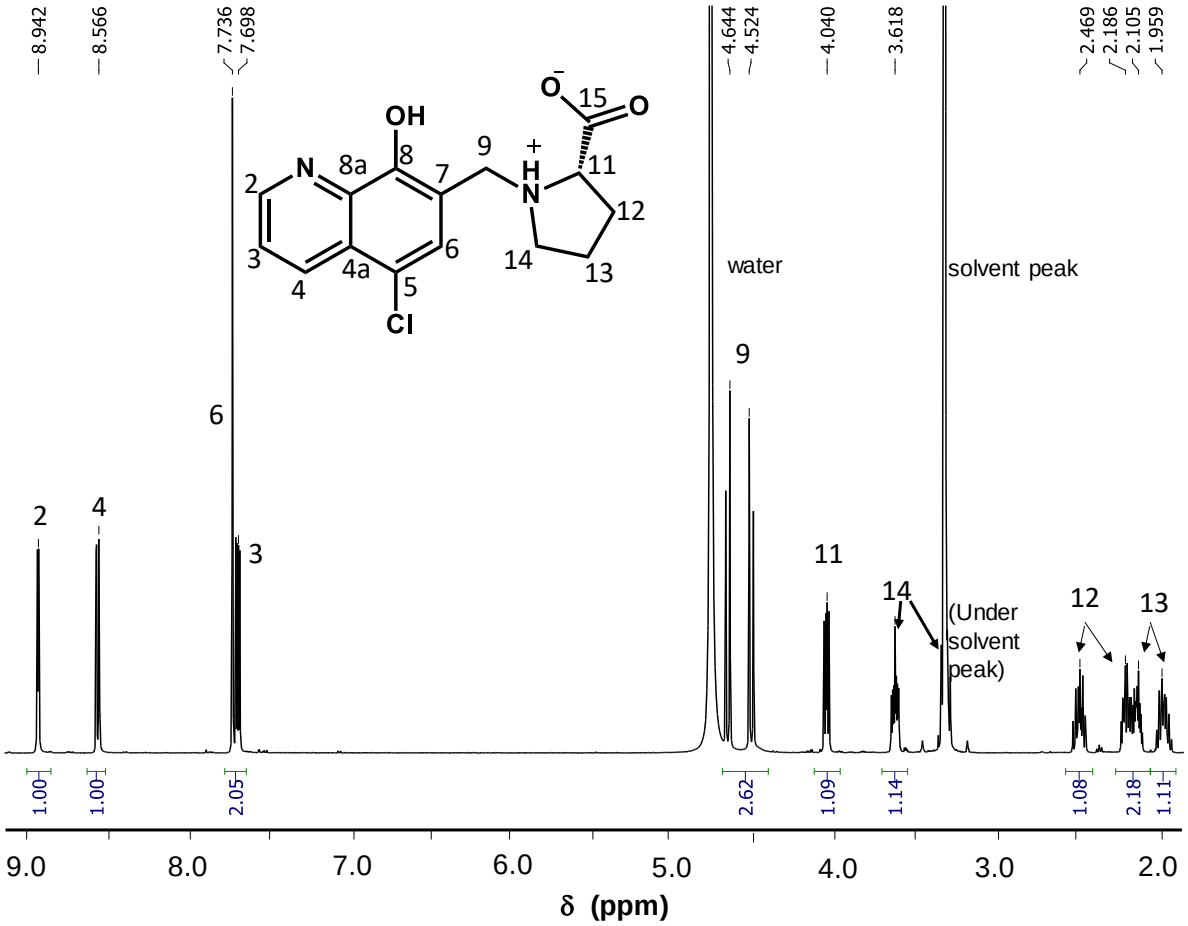

Fig. S2. ^{1}H NMR spectrum of HQCl-Pro in CD_3OD. Inserted structure shows numbering of peaks. {*c*(HQCl-Pro) = 10 mM, *T* = 25.0°C}

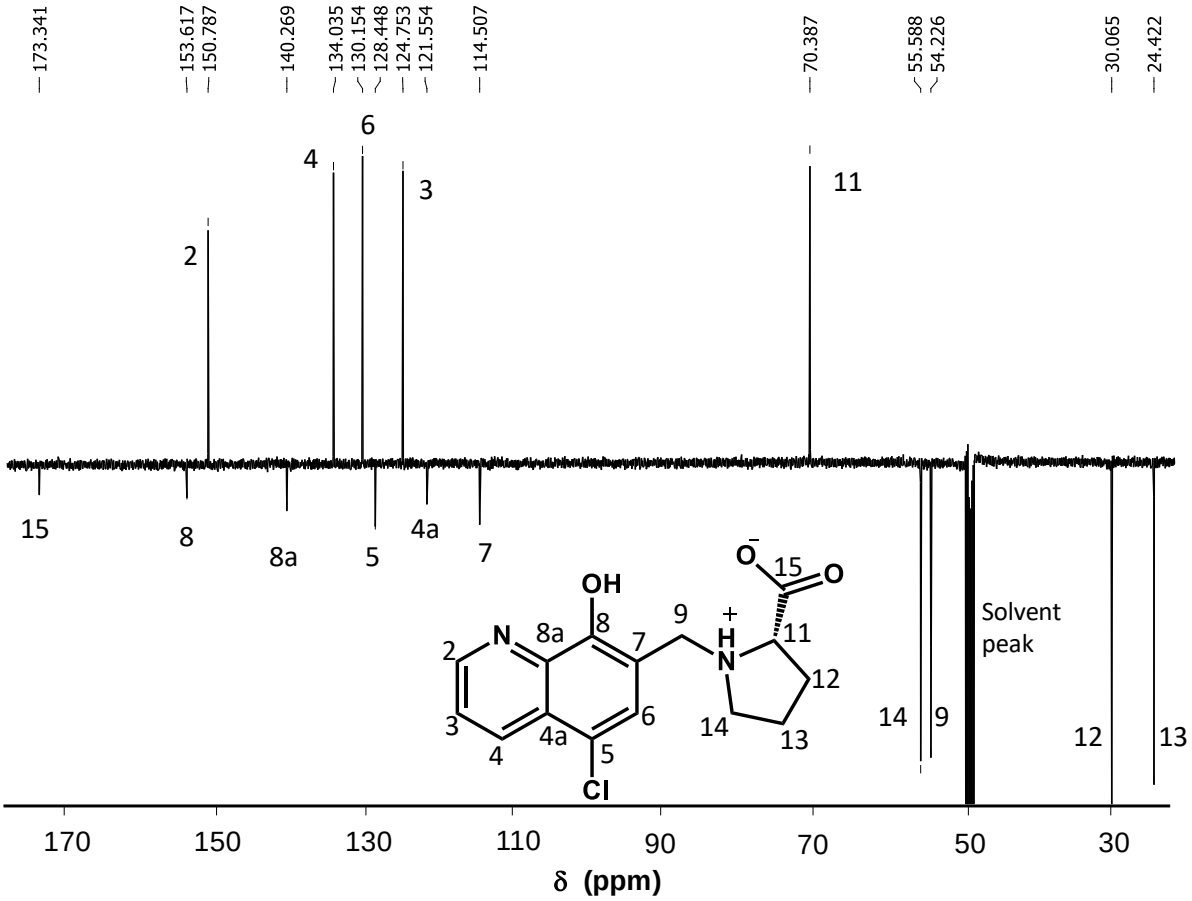

Fig. S3. ^{13}C APT NMR spectrum of HQCl-Pro in CD_3OD. Attached proton test method: CH and CH_3 peaks are positive, C and CH_2 peaks are negative. Inserted structure shows numbering of peaks. {*c*(HQCl-Pro) = 10 mM, *T* = 25.0°C}

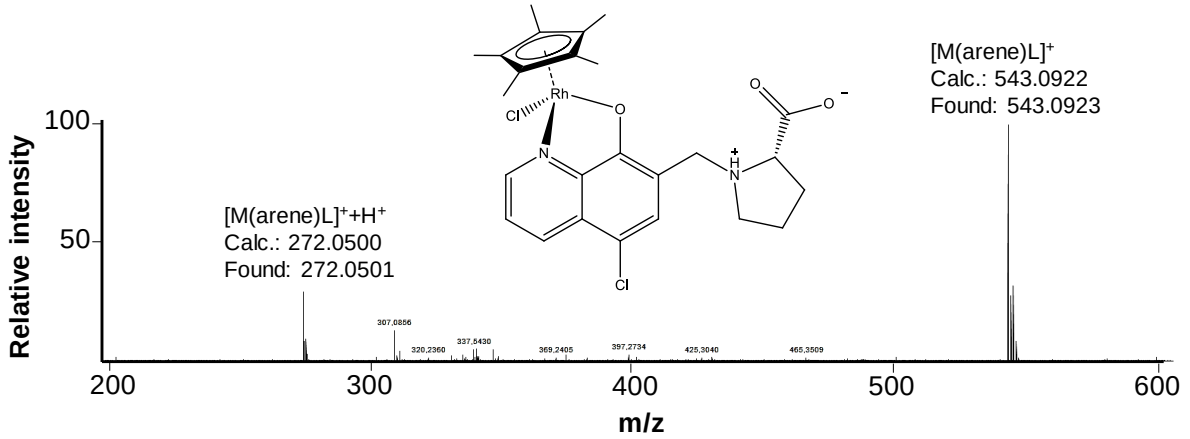

Fig. S4. ESI-MS spectrum of [Rh(η^5-C_5Me_5)(L)Cl] in positive mode.

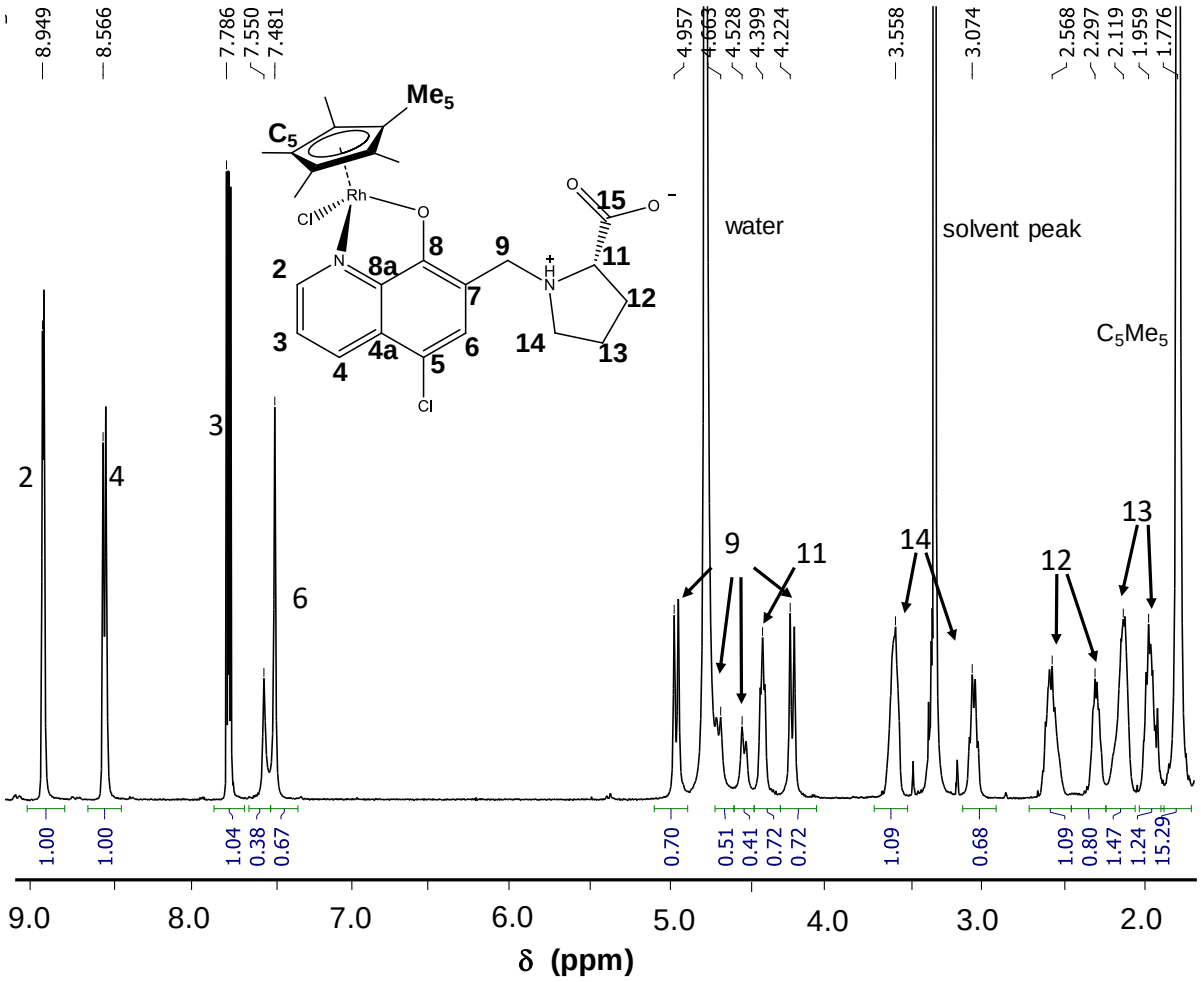

Fig. S5. ^{1}H NMR spectrum of [Rh(η^5-C_5Me_5)(L)Cl] in CD_3OD. Inserted structure shows numbering of peaks. {*c*([Rh(η^5-C_5Me_5)(L)Cl]) = 10 mM, *T* = 25.0°C}

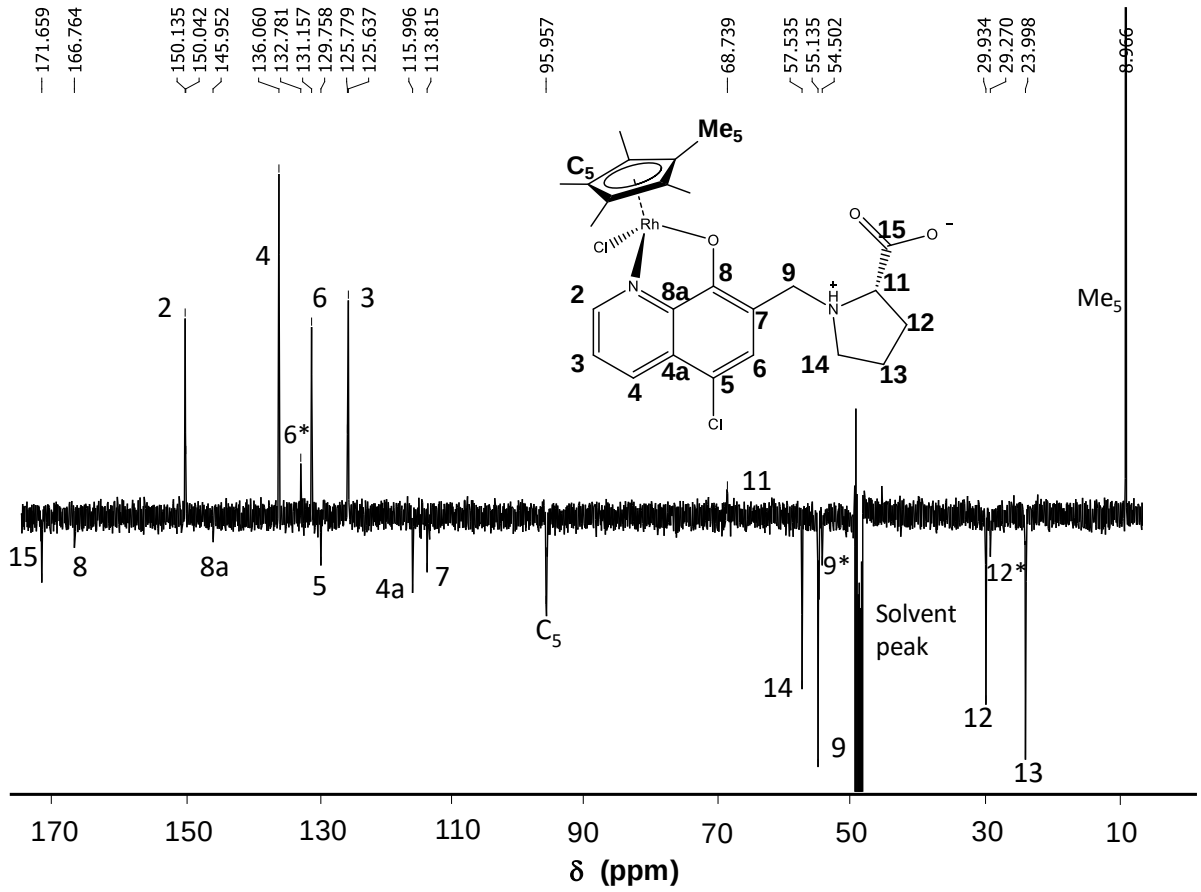

Fig. S6. ^{13}C APT NMR spectrum of [Rh(η^5-C_5Me_5)(L)Cl] in CD_3OD. Attached proton test method: CH and CH_3 peaks are positive, C and CH_2 peaks are negative. Inserted structure shows numbering of peaks. {*c*([Rh(η^5-C_5Me_5)(L)Cl]) = 10 mM, *T* = 25.0°C}

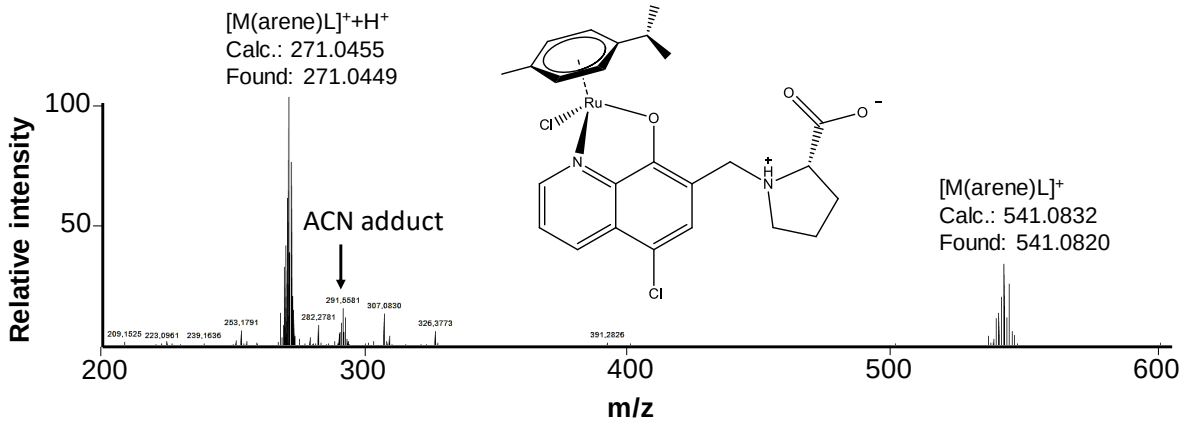

Fig. S7. ESI-MS spectrum of [Ru(η^6-*p*-cym)(L)Cl] in positive mode.

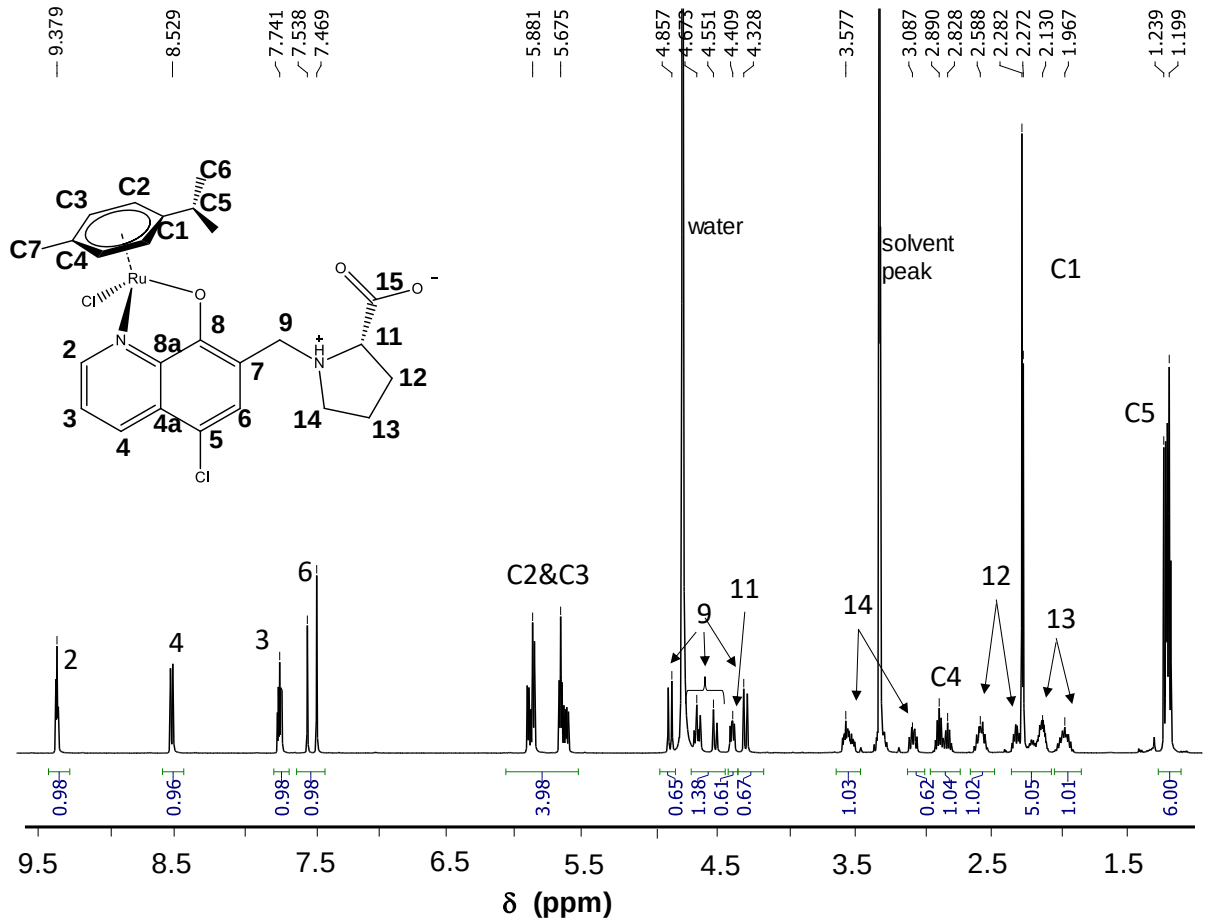

Fig. S8. ^{1}H NMR spectrum of [Ru(η^6-*p*-cym)(L)Cl] in CD_3OD. Inserted structure shows numbering of peaks. {*c*([Ru(η^6-*p*-cym)(L)Cl]) = 10 mM, *T* = 25.0°C}

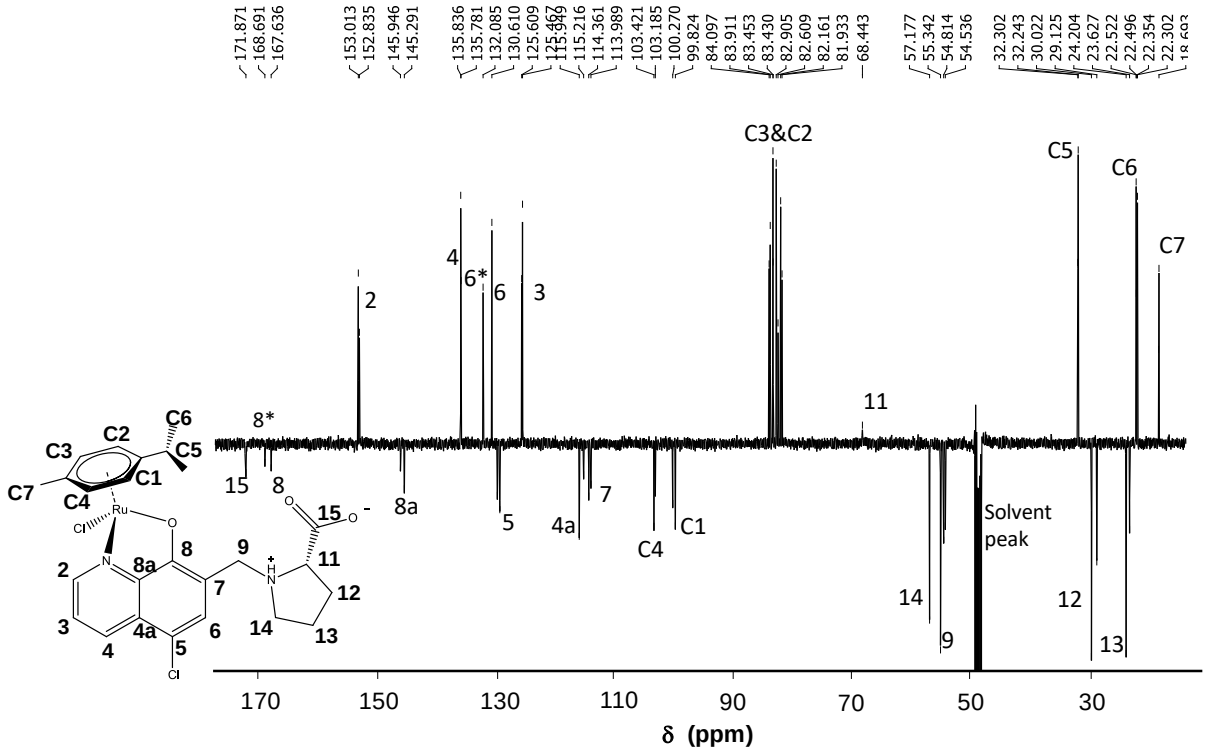

Fig. S9. ^{13}C APT NMR spectrum of [Ru(η^6-*p*-cym)(L)Cl] in CD_3OD. Attached proton test method: CH and CH_3 peaks are positive, C and CH_2 peaks are negative. Inserted structure shows numbering of peaks. {*c*([Ru(η^6-*p*-cym)(L)Cl]) = 10 mM, *T* = 25.0°C}

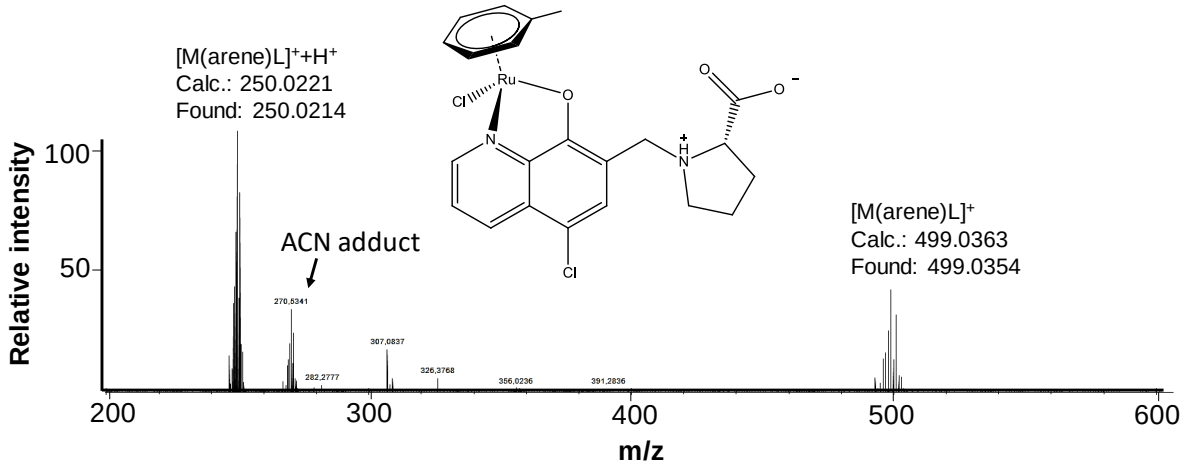

Fig. S10. ESI-MS spectrum of [Ru(η^6-tol)(L)Cl] in positive mode.

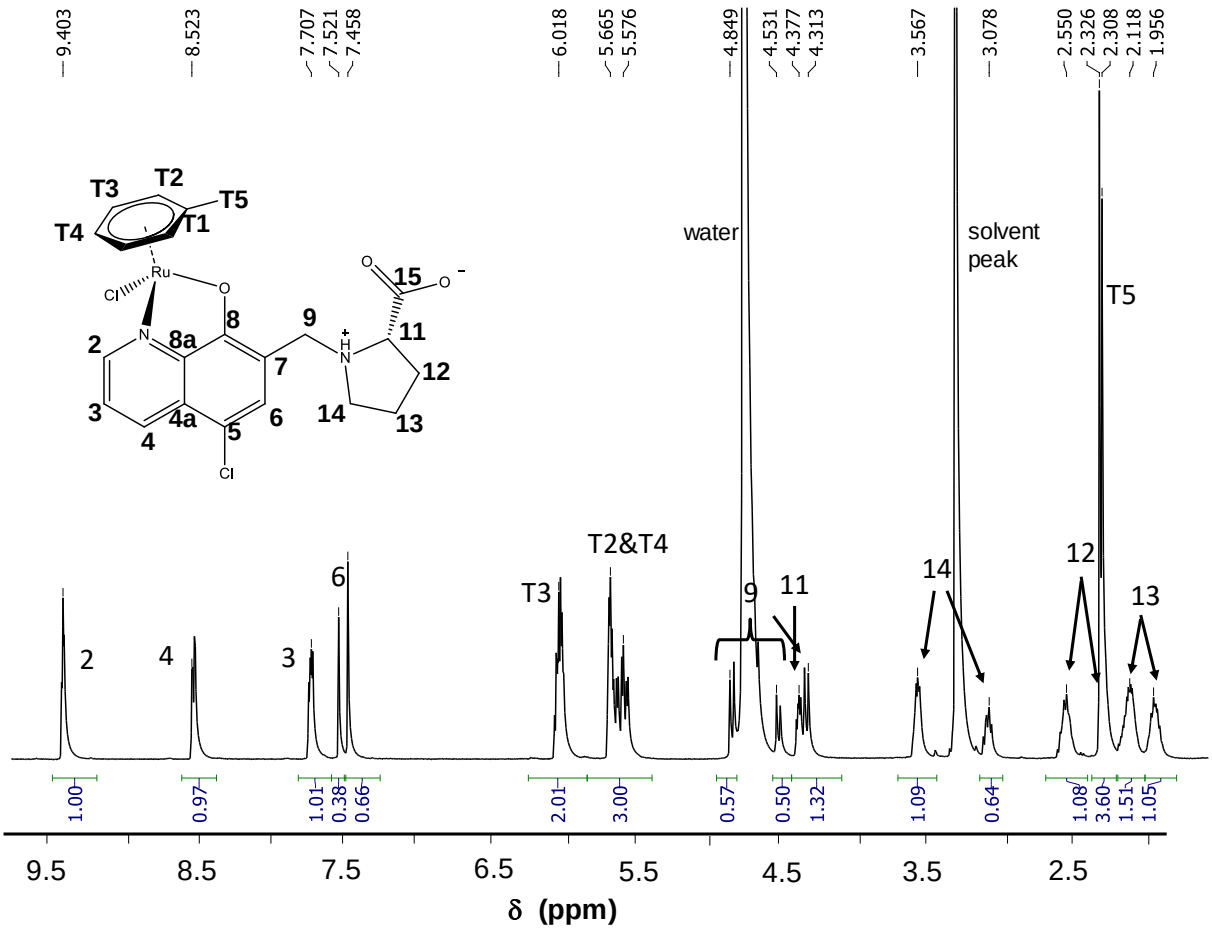

Fig. S11. ^{1}H NMR spectrum of [Ru(η^6-tol)(L)Cl] in CD_3OD. Inserted structure shows numbering of peaks. {*c*([Ru(η^6-tol)(L)Cl]) = 10 mM, *T* = 25.0°C}

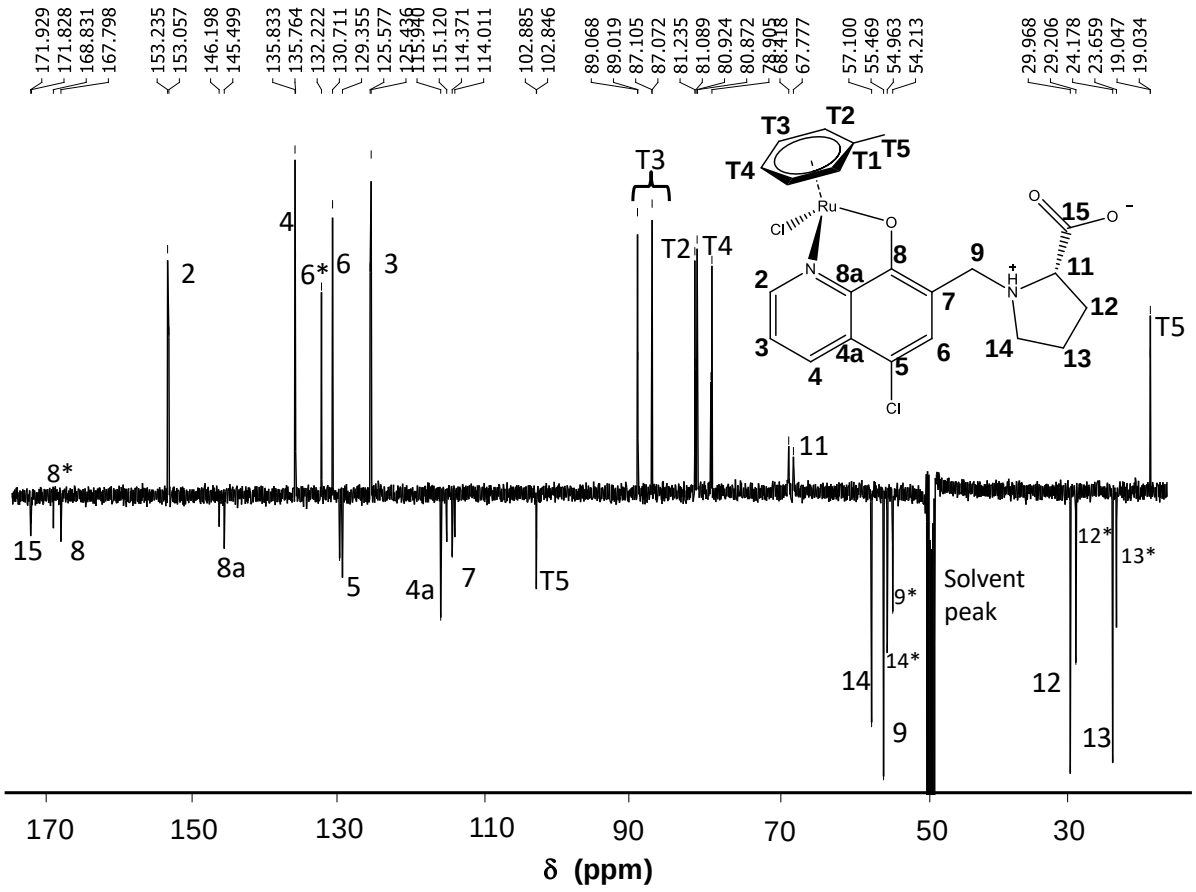

Fig. S12. ^{13}C APT NMR spectrum of [Ru(η^6-tol)(L)Cl] in CD_3OD. Attached proton test method: CH and CH_3 peaks are positive, C and CH_2 peaks are negative. Inserted structure shows numbering of peaks. {*c*([Ru(η^6-tol)(L)Cl]) = 10 mM, *T* = 25.0°C}

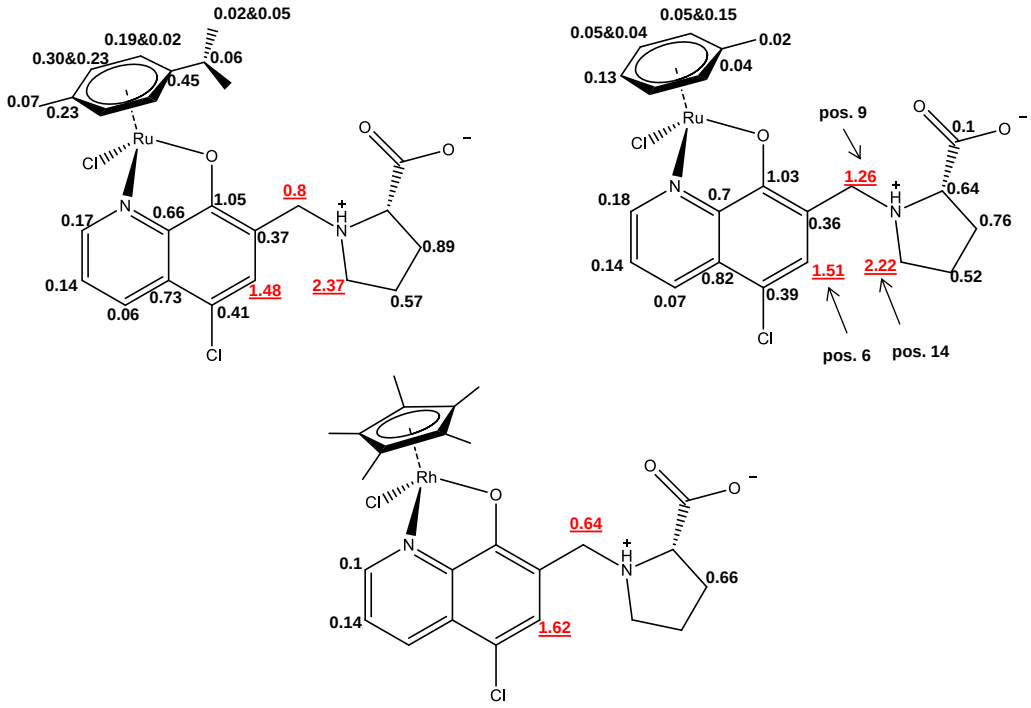

Fig. S13. Differences of peaks belonging to the same protons in the two sets of peaks detected in ^{13}C NMR spectra recorded for the complexes. Differences are projected on the proposed structures. Positions 6,9 and 14 (biggest differences) are highlighted. {c([Ru(η^6-tol)(L)Cl]) = 10 mM, T = 25.0°C}

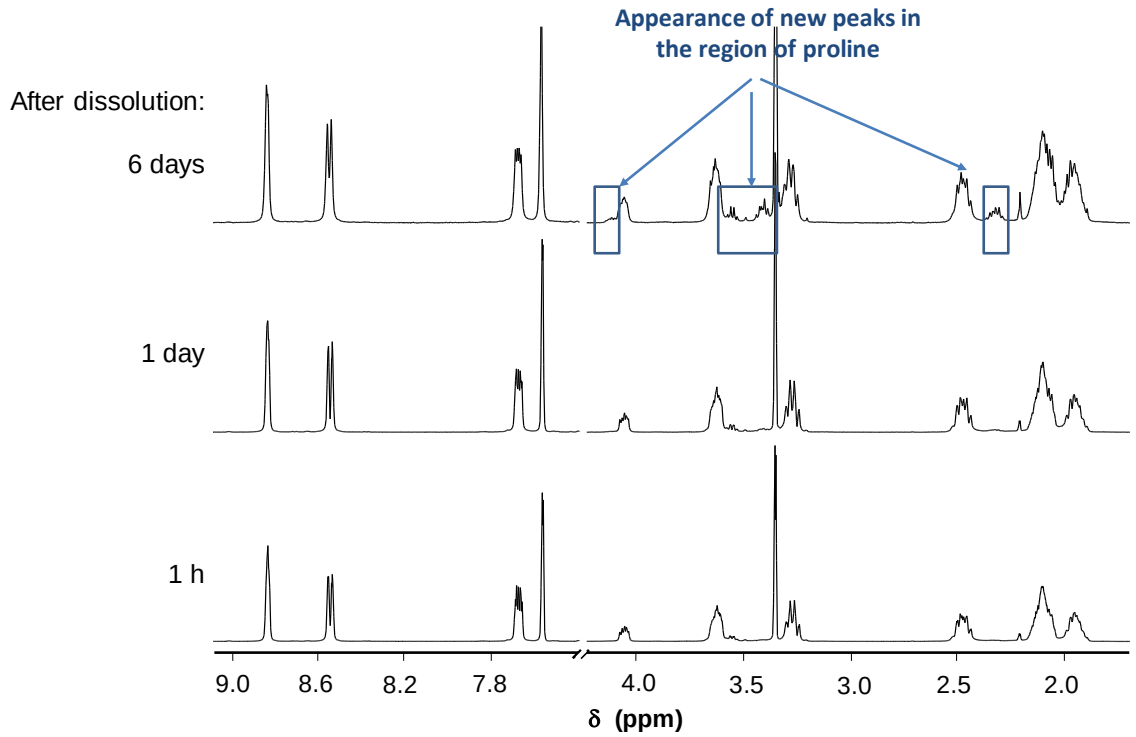

Fig. S14. Monitoring the stability of HQCl-Pro ligand in phosphate buffer at pH = 7.4 by ^1H NMR spectroscopy. New set of aliphatic peaks are signed with blue rectangles. {c(HQCl-Pro) = 10 mM; solvent: 90% H_2O / 10% D_2O; pH = 7.40 (phosphate buffer); T = 25.0 °C}

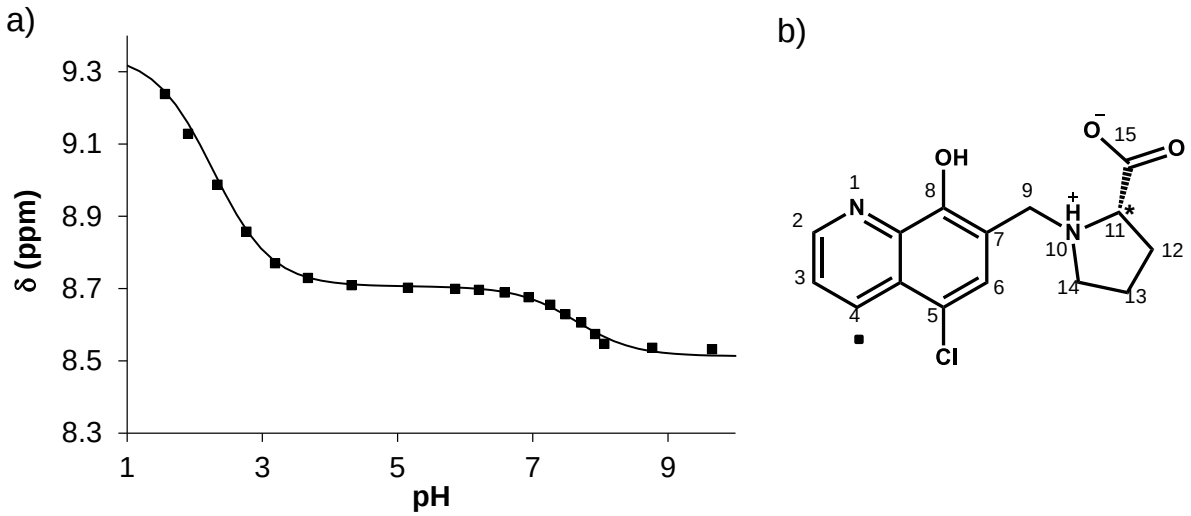

Fig. S15. a) Measured and fitted chemical shift values of C^4H proton at pH = 1.5-10.0. b) Numbering of HQCl-Pro, C^4H is highlighted. {*c*(HQCl-Pro) = 480 μM; solvent: 90% H_2O / 10% D_2O; *T* = 25.0 °C; *I* = 0.20 M (KNO_3)}

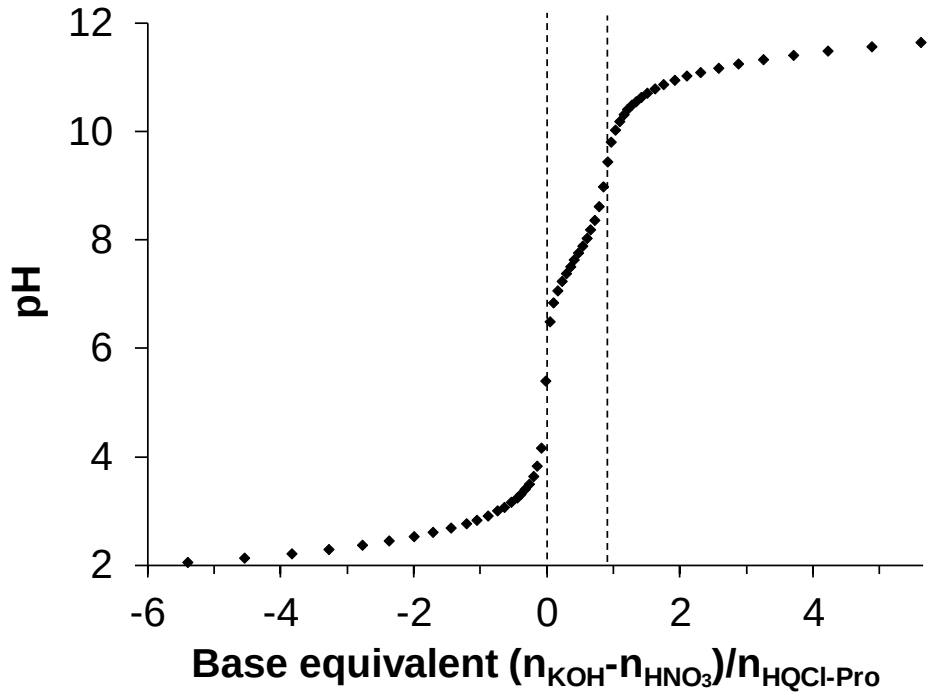

Fig. S16. Representative pH-potentiometric curve for the ligand HQCl-Pro. Negative base equivalent values mean excess of acid. {*c*(HQCl-Pro) = 2 mM; *I* = 0.20 M (KNO_3); *T* = 25.0 °C}

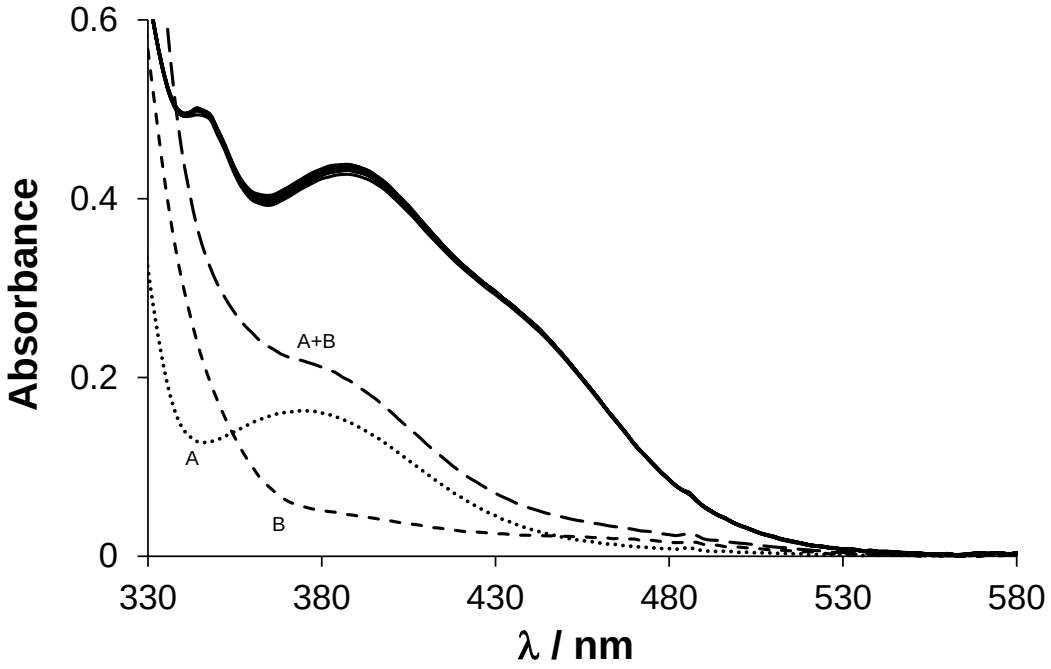

Fig. S17. Time-dependent UV-Vis absorption spectra of the Rh(η^5-C_5Me_5) – HQCl-Pro system at pH = 3.56 (solid lines). Dotted curve shows the absorption spectrum of organometallic ion (A), dashed curve shows the spectrum of HQCl-Pro (B), long dashed curve shows their additive spectrum (A+B). {c([Rh(η^5-C_5Me_5)$(H_2O)_3$]$^{2+}$) = c(HQCl-Pro) = 110 μM; pH = 3.56; I = 0.20 M (KNO_3); T = 25.0 °C; ℓ = 1 cm}

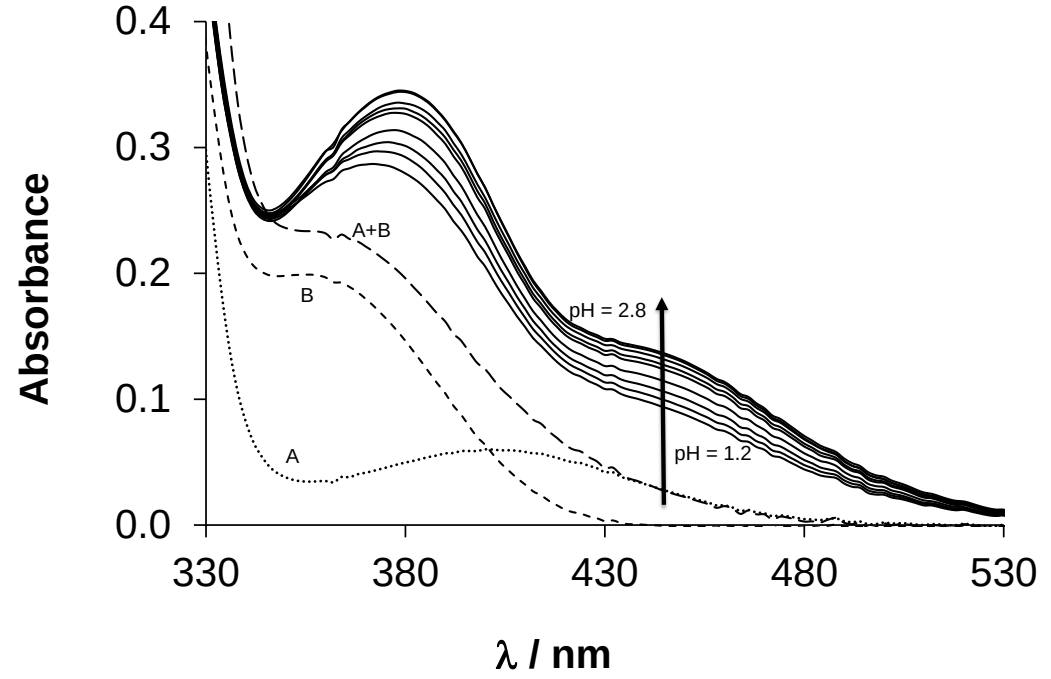

Fig. S18. UV-Vis absorption spectra of the Ru(η^6-tol) – HQ system at pH = 1.2-2.8 (solid lines). Dotted curve shows the absorption spectrum of metal ion (A), dashed curve shows HQ ligand spectrum (B), long dashed curve shows their additive spectrum (A+B). {c([Ru(η^6-tol)$(H_2O)_3$]$^{2+}$) = c(HQ) = 110 μM; I = 0.20 M (KNO_3); T = 25.0 °C; ℓ = 1 cm}

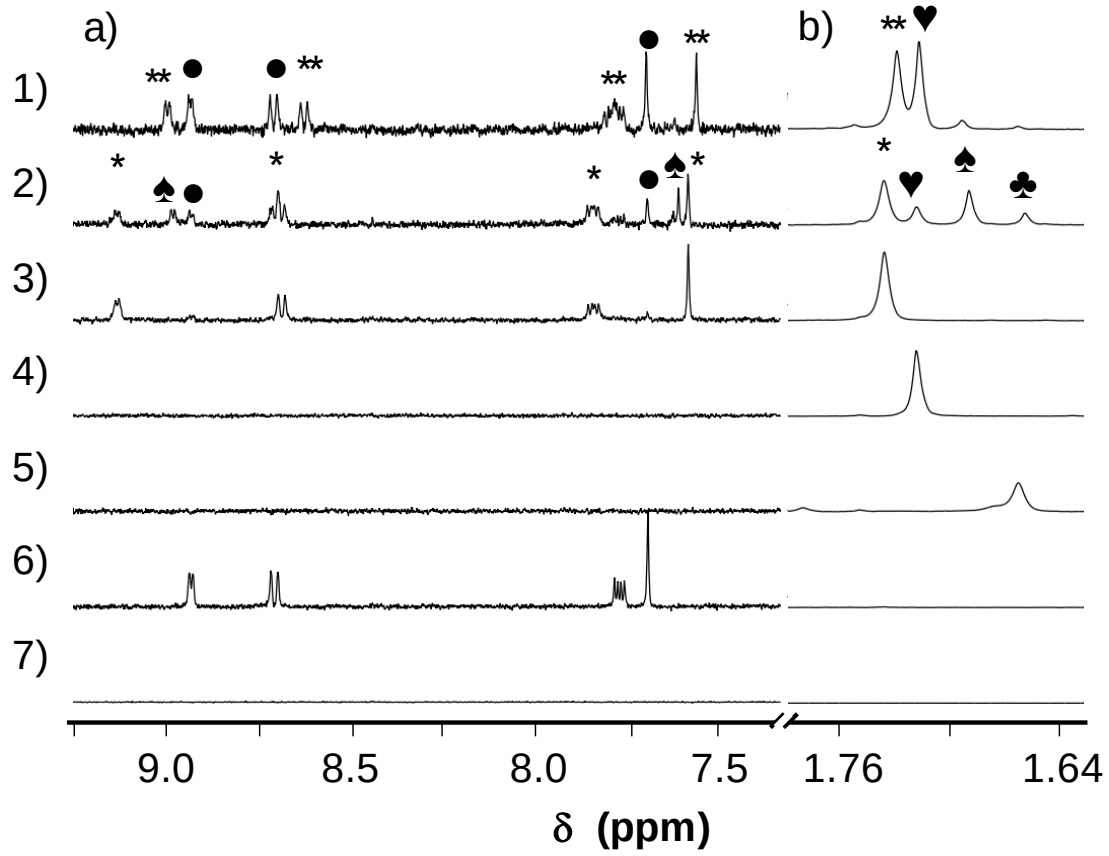

Fig. S19. Monitoring of HQCl-Pro displacement from $[Rh(\eta^5\text{-}C_5Me_5)(L)(H_2O)]^+$ (where L is the coordinated form of HQCl-Pro) with 1,2-ethylenediamine by ^1H NMR spectroscopy. a) aromatic region b) aliphatic region.

1) $[Rh(\eta^5\text{-}C_5Me_5)(L)(H_2O)]^+$: ethylenediamine = 1:23, I = 0.20 M (KCl);

2) $[Rh(\eta^5\text{-}C_5Me_5)(L)(H_2O)]^+$: ethylenediamine = 1:23;

3) $[Rh(\eta^5\text{-}C_5Me_5)(L)(H_2O)]^+$;

4) $[Rh(\eta^5\text{-}C_5Me_5)(H_2O)_3]^{2+}$: ethylenediamine = 1:23;

5) $[Rh(\eta^5\text{-}C_5Me_5)(H_2O)_3]^{2+}$;

6) free HQCl-Pro;

7) free ethylenediamine.

Peak assignment: free HQCl-Pro (●); $[Rh(\eta^5\text{-}C_5Me_5)(HQCl\text{-}Pro)(H_2O)]^+$ (*); $[Rh(\eta^5\text{-}C_5Me_5)(HQCl\text{-}Pro)(Cl)]$ (**); $[Rh(\eta^5\text{-}C_5Me_5)(en)(H_2O)]^{2+}$ (♥); mixed ligand complexes (♠ and ♣).

{$c([Rh(\eta^5\text{-}C_5Me_5)(H_2O)_3]^{2+})$ = c(HQCl-Pro) = 100 μM; c(ethylenediamine) = 2.34 mM; solvent: 90% H_2O / 10% D_2O; pH = 6.14 (20 mM phosphate buffer); T = 25.0 °C; t = 24 h}

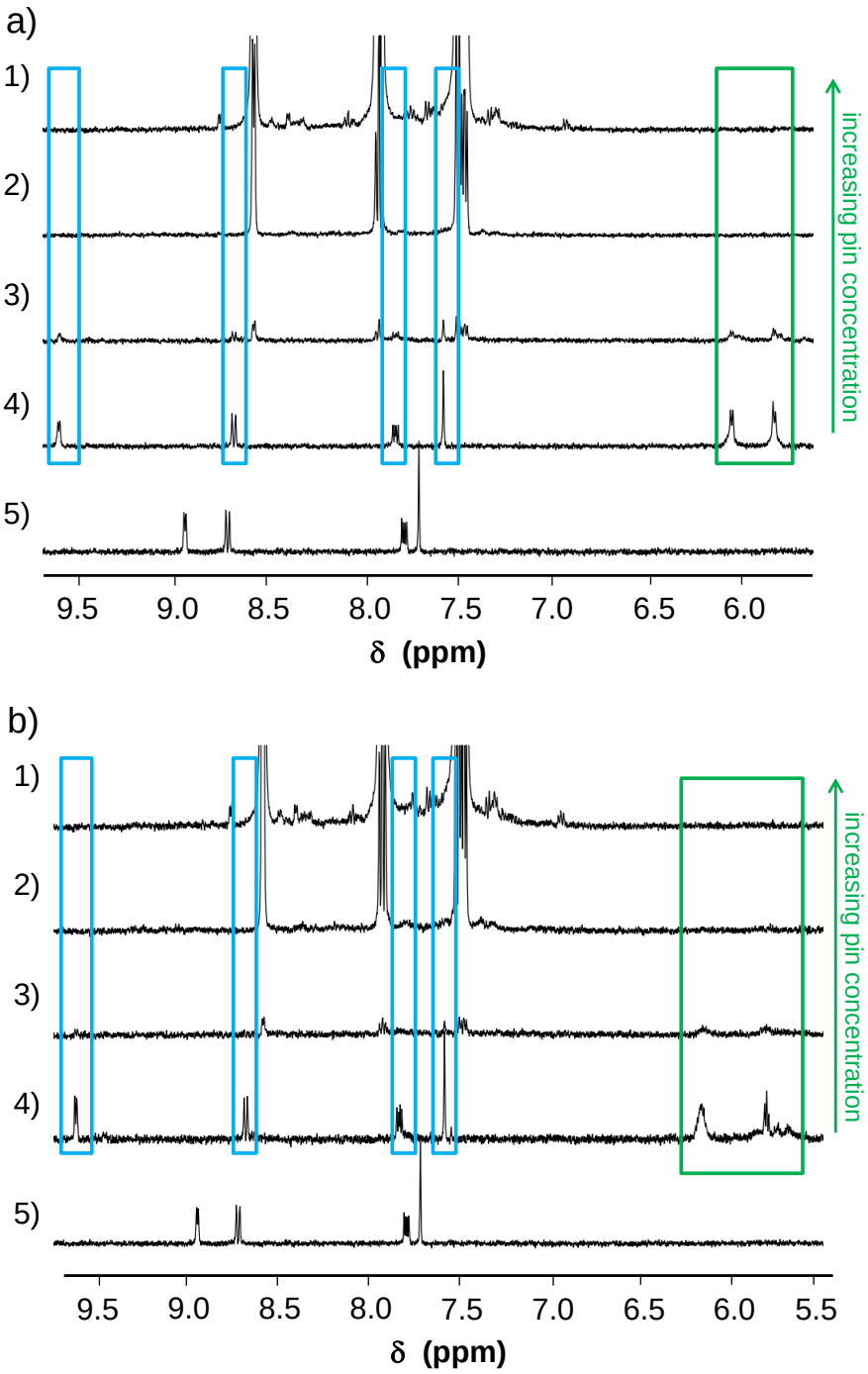

Fig. S20. Monitoring of arene loss at high excess of 2-picolylamine by ^{1}H NMR spectroscopy. Arene: a) *p*-cymene and b) toluene.

1) $[Ru(\eta^6\text{-arene})(L)(H_2O)]^+$: pin = 1:82; (L: coordinated form of HQCl-Pro)

2) $[Ru(\eta^6\text{-arene})(L)(H_2O)]^+$: pin = 1:11;

3) $[Ru(\eta^6\text{-arene})(L)(H_2O)]^+$: pin = 1:1;

4) $[Ru(\eta^6\text{-arene})(L)(H_2O)]^+$ in buffer;

5) HQCl-Pro in buffer.

Blue rectangle: the coordinated HQCl-Pro's aromatic peaks; green rectangle: the arenes' aromatic protons. {$c([Ru(\eta^6\text{-arene})(H_2O)_3]^{2+})$ = c(HQCl-Pro) = 100 μM; c(2-picolylamine) = 100 μM- 8.2 mM; solvent: 90% H_2O / 10% D_2O; pH = 6.0 (20 mM phosphate buffer); T = 25.0 °C; t = 24 h}

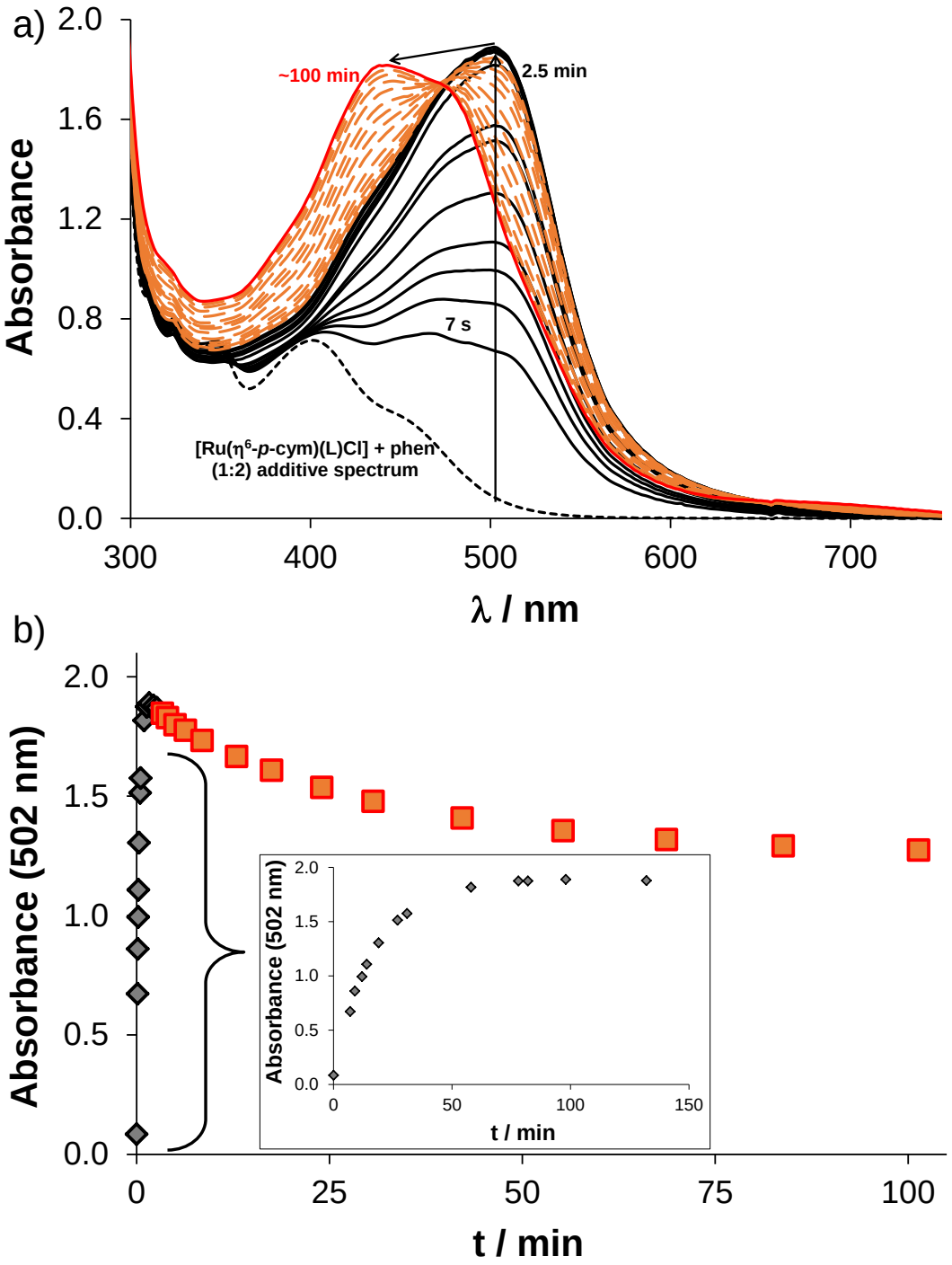

Fig. S21. a) Time-dependent UV-Vis absorption spectra of the $[Ru(\eta^6\text{-}p\text{-cym})(L)(H_2O)]^+$ – 1,10-phenanthroline (1:2) system at pH = 7.40, in the presence of O_2 (L: coordinated form of HQCl-Pro). Dashed curve shows the additive spectrum of the metal complex and 2 eqs of 1,10-phenanthroline. b) Absorbance values at 502 nm in the function of time. Inset shows the completed first step in the first 150 seconds. {$c([Ru(\eta^6\text{-}p\text{-cym})(L)(H_2O)]^+)$ = 200 μM; c(1,10-phenanthroline) = 400 μM; pH = 7.40 (20 mM phosphate; c(KCl) = 0.10 M; T = 25.0 °C; ℓ = 1 cm}

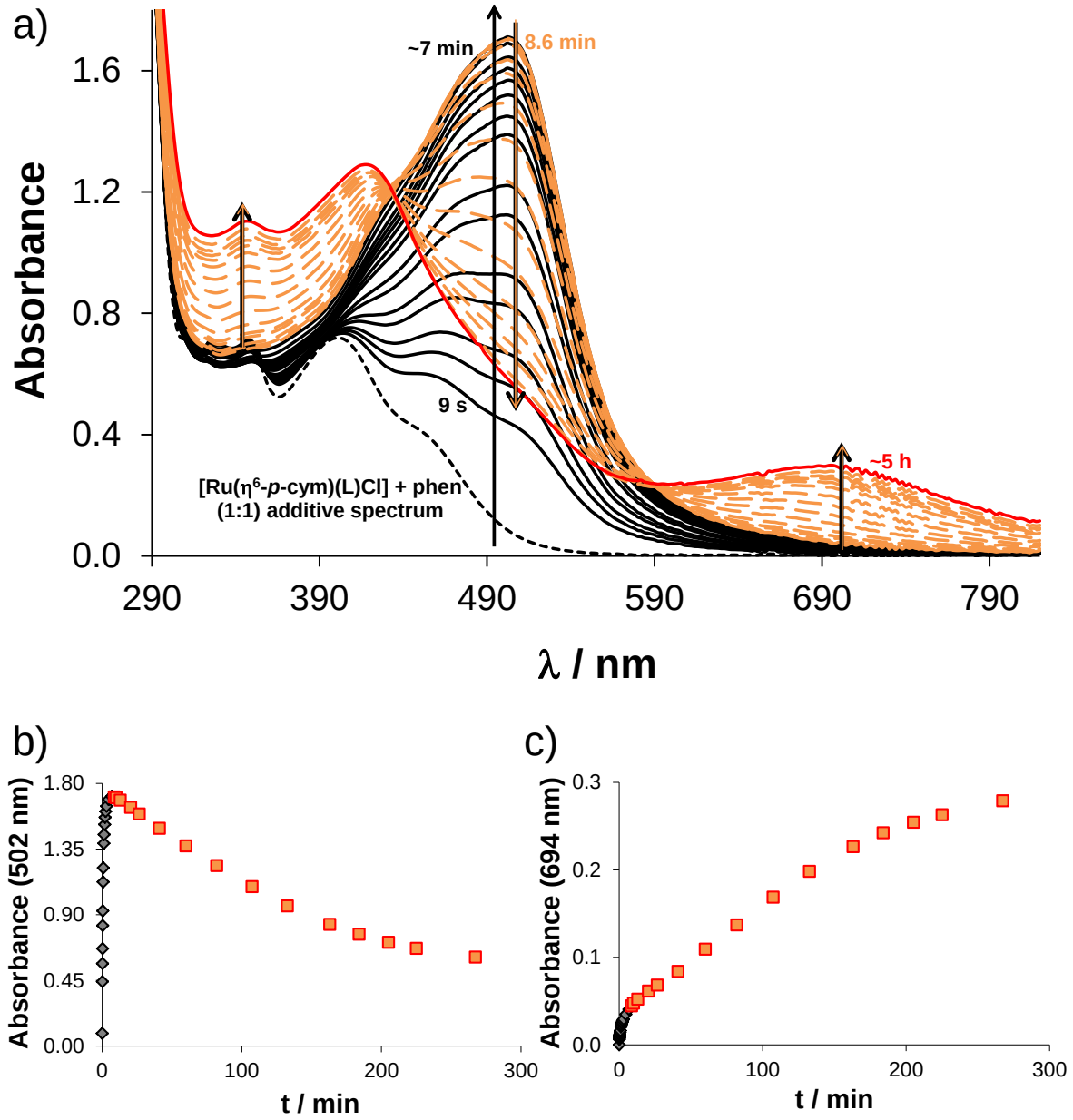

Fig. S22. a) Time-dependent UV-Vis absorption spectra of the $[Ru(\eta^6\text{-}p\text{-cym})(L)(H_2O)]^+$ – 1,10-phenanthroline (1:1) system at pH = 7.40, in the presence of O_2 (L: coordinated form of HQCl-Pro). Dashed curve shows the additive spectrum of the metal complex and 1 eq of 1,10-phenanthroline. b) Absorbance values at 502 nm in the function of time. c) Absorbance values at 694 nm in the function of time. {$c([Ru(\eta^6\text{-}p\text{-cym})(L)(H_2O)]^+)$ = 200 μM; c(1,10-phenanthroline) = 200 μM; pH = 7.40 (20 mM phosphate; c(KCl) = 0.10 M; T = 25.0 °C; ℓ = 1 cm}

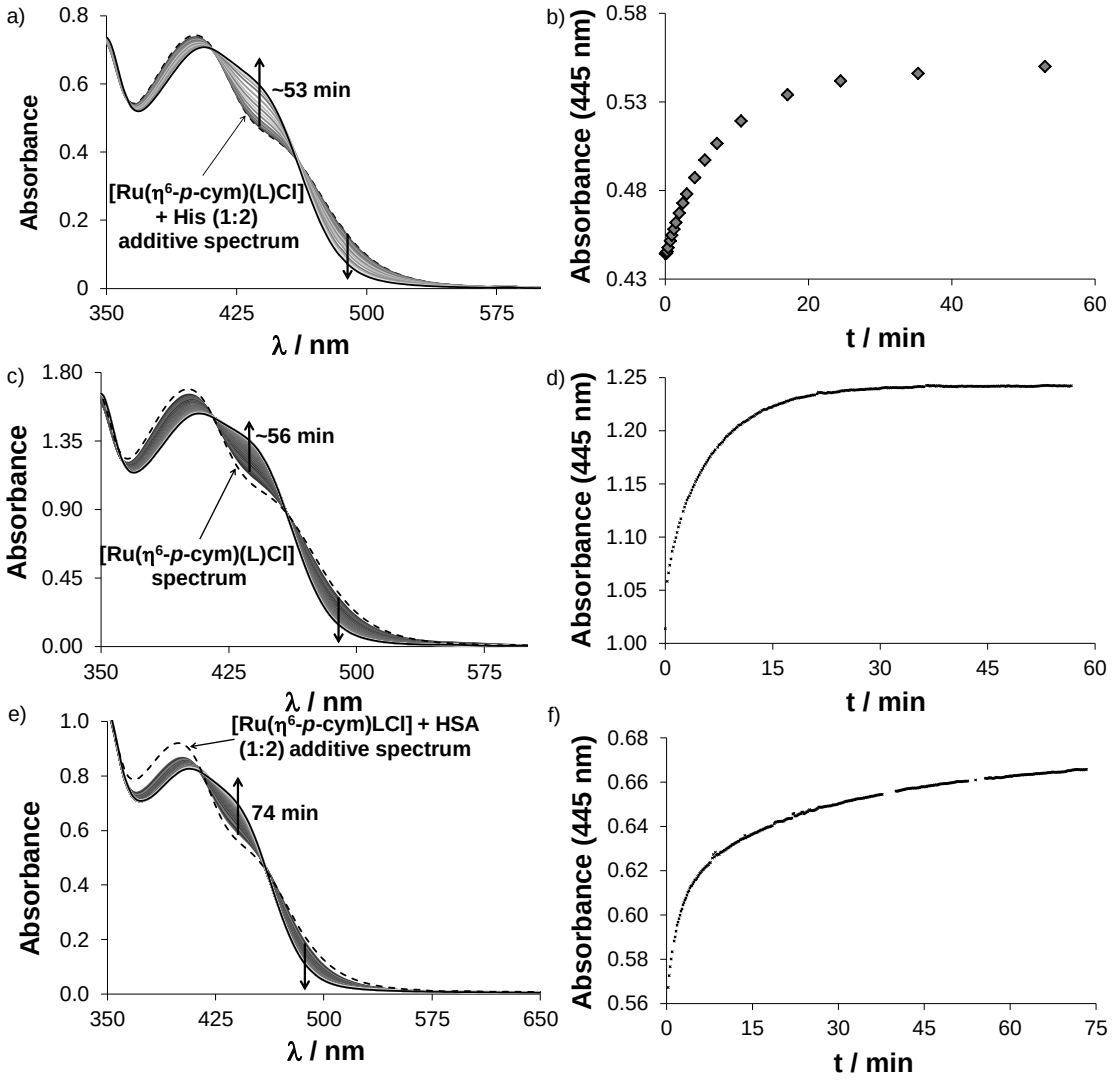

Fig. S23. Time-dependent UV-Vis absorption spectra of the a) $[Ru(\eta^6\text{-}p\text{-cym})(L)(H_2O)]^+$ – L-histidine (1:2); c) $[Ru(\eta^6\text{-}p\text{-cym})(L)(H_2O)]^+$ – RPMI 1640; e) $[Ru(\eta^6\text{-}p\text{-cym})(L)(H_2O)]^+$ – human serum albumin (HSA) (1:2) systems at pH = 7.40, under aerobic conditions (L: coordinated form of HQCl-Pro). Dashed curves show the additive spectrum of the metal complex and 2 eqs of His/HSA. b,d,f). Absorbance values at 445 nm in the function of time. {$c([Ru(\eta^6\text{-}p\text{-cym})(L)(H_2O)]^+)$ = 200 μM (or 400 μM (in c,d)); c(His) = 400 μM; c(HSA) = 400 μM; pH = 7.40 (20 mM phosphate or RPMI 1640 itself); c(KCl) = 0.10 M; T = 25.0 °C; ℓ = 1 cm}

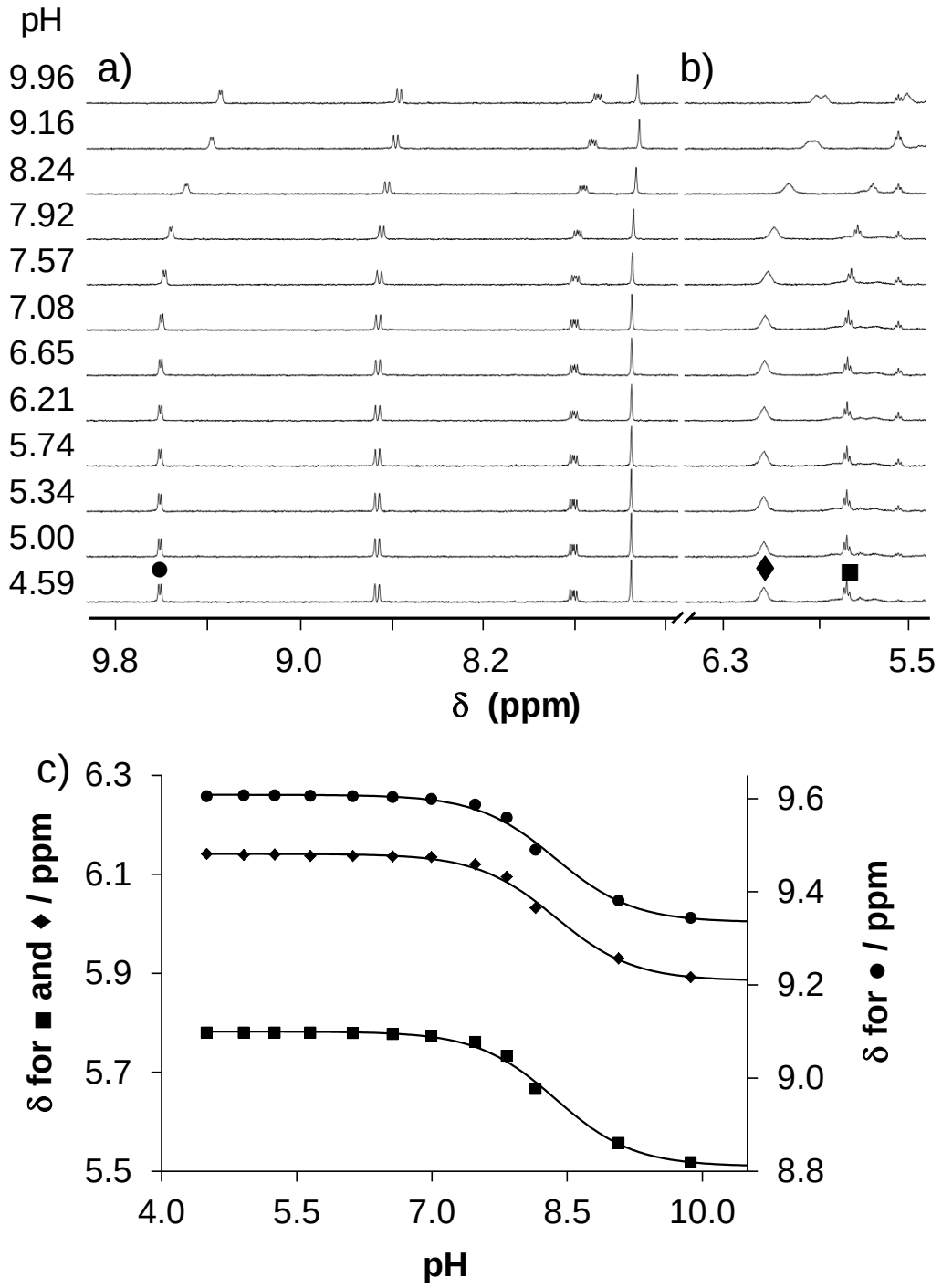

Fig. S24. ^{1}H NMR spectra of the Ru(η^6-tol) – HQCl-Pro 1:1 system recorded at pH = 4.6-10.0. a) HQCl-Pro aromatic protons b) toluene aromatic protons. c) Measured (●,♦ and ■) and fitted (solid lines) chemical shift values of HQCl-Pro and toluene aromatic protons in the function of pH. {c(Ru(η^6-tol)$(H_2O)_3]^{2+}$) = c(HQCl-Pro) = 300 μM; solvent: 90% H_2O / 10% D_2O; T = 25.0 °C; I = 0.20 M (KNO_3)}

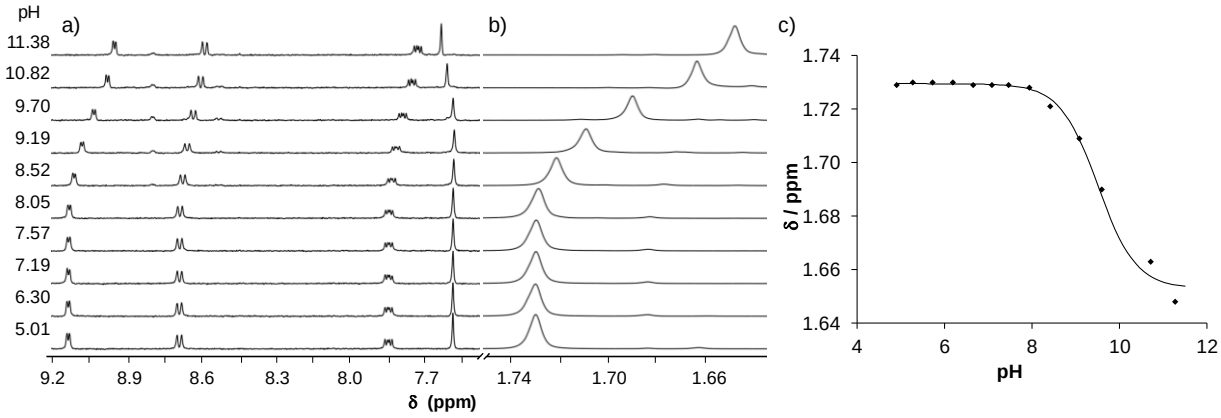

Fig. S25. ^{1}H NMR spectra of the Rh(η^5-C_5Me_5) – HQCl-Pro 1:1 system recorded at pH = 5.0-11.4. a) Aromatic region (with increased intensity) b) C_5Me_5 methyl protons. c) Measured (♦) and fitted (solid line) chemical shift values of the methyl groups of C_5Me_5 in the function of pH. {c(Rh(η^5-C_5Me_5)$(H_2O)_3]^{2+}$) = c(HQCl-Pro) = 300 μM; solvent: 90% H_2O / 10% D_2O; T = 25.0 °C; I = 0.20 M (KNO_3)}

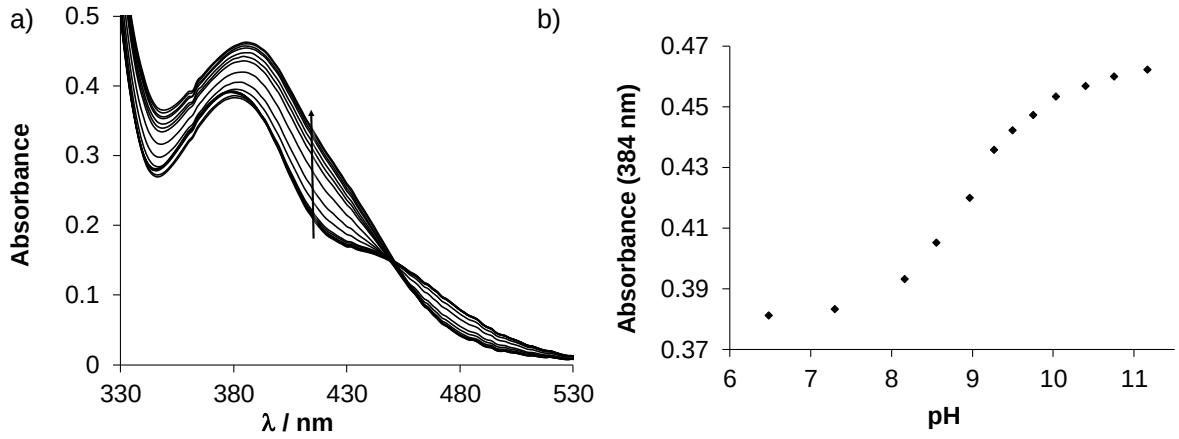

Fig. S26. a) UV-Vis absorption spectra of [Ru(η^6-tol)(8-hydroxyquinolato)$(H_2O)]^+$ at pH = 2.0-11.5. b) Measured absorbance values at 384 nm.{c([Ru(η^6-tol)$(H_2O)_3]^{2+}$) = c(HQ) = 130 μM; T = 25.0 °C; I = 0.20 M (KNO_3); ℓ = 1 cm}

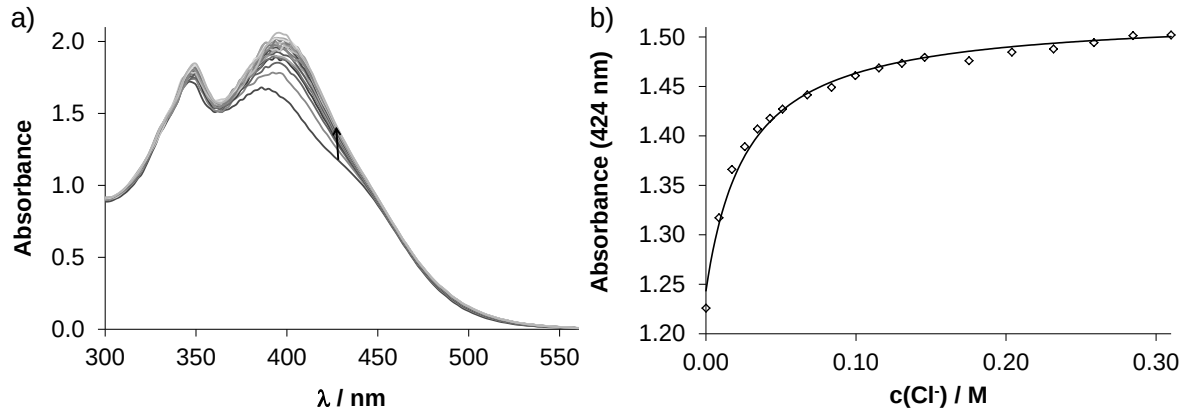

Fig. S27. a) UV-Vis absorption spectra of $[Rh(\eta^5\text{-}C_5Me_5)(L)(H_2O)]^+$ (L: coordinated form of HQCl-Pro) in the presence of chloride ions at different concentrations. b) Measured (◊) and fitted (solid line) absorbance values at 424 nm.{$c([Rh(\eta^5\text{-}C_5Me_5)(H_2O)_3]^{2+})$ = c(HQCl-Pro) = 400 μM; $c(Cl^-)$ = 0 – 310 mM; pH = 5.52 (phosphate buffer); T = 25.0 °C; ℓ = 1 cm}

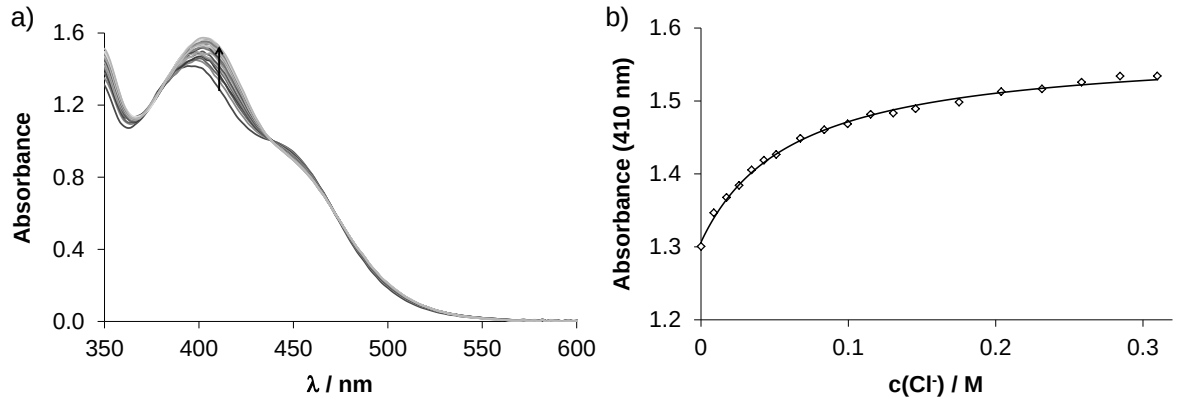

Fig. S28. a) UV-Vis absorption spectra of $[Ru(\eta^6\text{-}p\text{-cym})(L)(H_2O)]^+$ (L: coordinated form of HQCl-Pro) in the presence of chloride ions at different concentrations. b) Measured (◊) and fitted (solid line) absorbance values at 410 nm.{$c([Ru(\eta^6\text{-}p\text{-cym})(H_2O)_3]^{2+})$ = c(HQCl-Pro) = 400 μM; $c(Cl^-)$ = 0 – 310 mM; pH = 5.42 (phosphate buffer); T = 25.0 °C; ℓ = 1 cm}

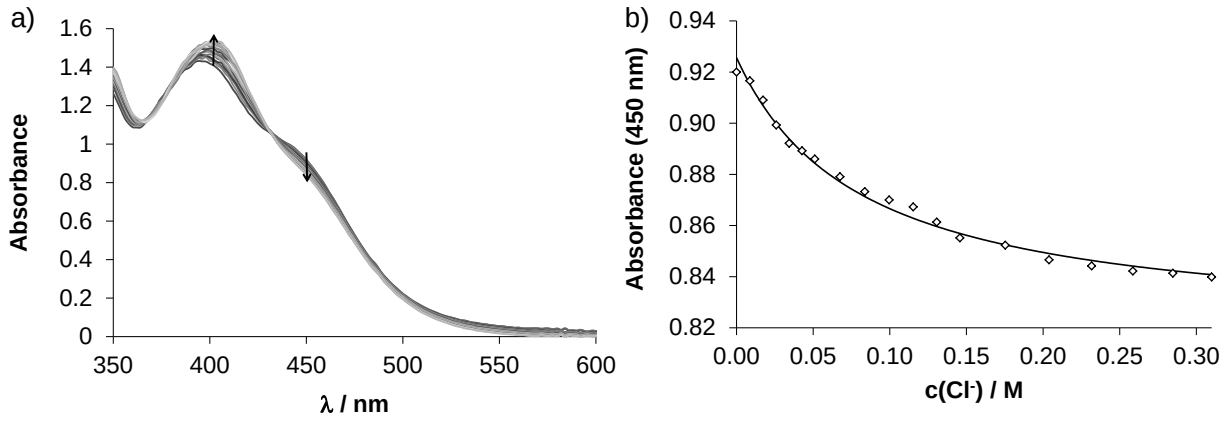

Fig. S29. a) UV-Vis absorption spectra of complex $[Ru(\eta^6\text{-tol})(L)(H_2O)]^+$ in the presence of chloride ions at different concentrations (L is the coordinated form of HQCl-Pro). b) Measured (◊) and fitted (solid line) absorbance values at 450 nm. {$c([Ru(\eta^6\text{-tol})(H_2O)_3]^{2+}$) = c(HQCl-Pro) = 400 μM; $c(Cl^-)$ = 0- 310 mM; pH = 5.46 (phosphate buffer); T = 25.0 °C; ℓ = 1 cm}

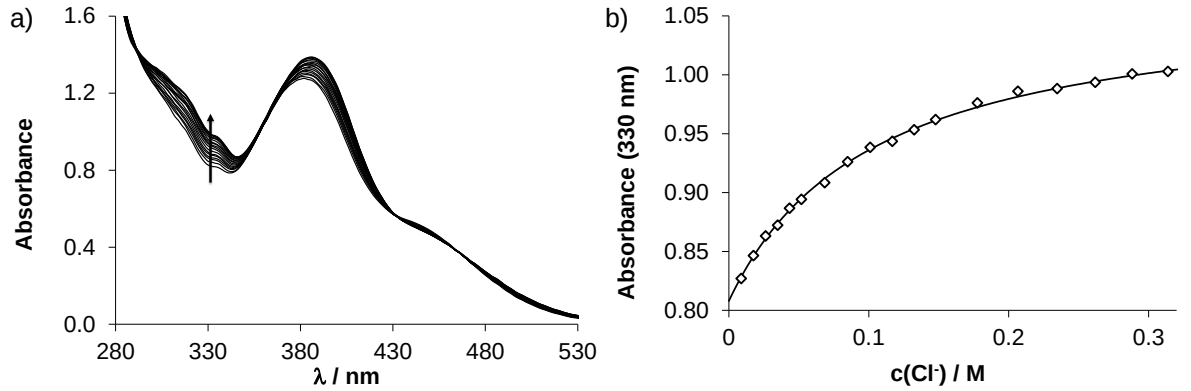

Fig. S30. a) UV-Vis absorption spectra of $[Ru(\eta^6\text{-tol})(8\text{-hydroxyquinolato})(H_2O)]^+$ in the presence of chloride ions at different concentrations. b) Measured (◊) and fitted (solid line) absorbance values at 330 nm.{$c([Ru(\eta^6\text{-tol})(H_2O)_3]^{2+}$) = c(HQ) = 400 μM; $c(Cl^-)$ = 0 – 310 mM; pH = 5.46 (phosphate buffer); T = 25.0 °C; ℓ = 1 cm}

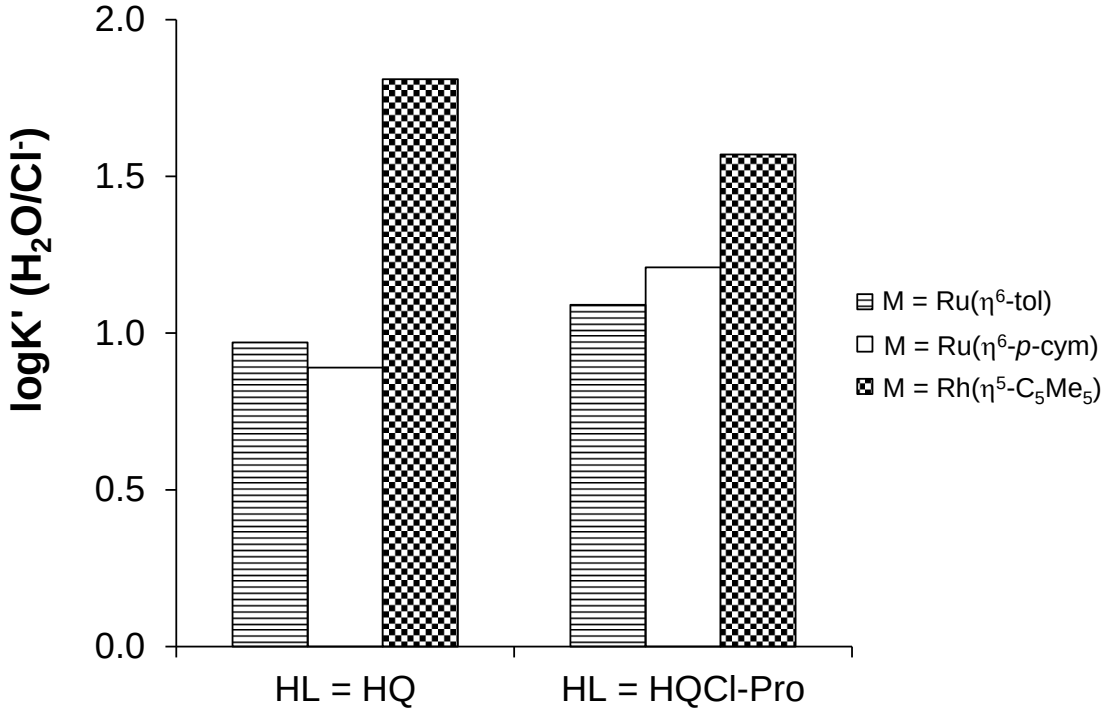

Fig. S31. Comparison of the log *K'* (H_2O/Cl^-) constants of half-sandwich 8-hydroxyquinolato complexes with the general structure: $[M(\eta^{5/6}\text{-arene})(L)(H_2O)]^+$. The constants for $[Ru(\eta^6\text{-tol})(8\text{-hydroxyquinolinato})(H_2O)]^+$ (0.99(1), Fig. S30) and for the HQCl-Pro complexes (Table 2) were determined in this work, for the other constants see Ref. 6.

REFERENCES

1. P. Gans, A. Sabatini and A. Vacca, Talanta, 1996, 43, 1739. https://doi.org/10.1016/0039-9140(96)01958-3
2. O. Dömötör, S. Aicher, M. Schmidlehner, M. S. Novak, A. Roller, M. A. Jakupec, W. Kandioller, C. G. Hartinger, B. K. Keppler and É. A. Enyedy, J. Inorg. Biochem., 2014, 134, 57. https://doi.org/10.1016/j.jinorgbio.2014.01.020
3. L. Bíró, A. J. Godó, Z. Bihari, E. Garribba and P. Buglyó, Eur. J. Inorg. Chem., 2013, 2013, 3090. https://doi.org/10.1002/ejic.201201527
4. H. M. Irving, M. G. Miles and L. D. Petit, Anal. Chim. Acta, 1967, 38, 475. https://doi.org/10.1016/S0003-2670(01)80616-4
5. SCQuery, The IUPAC Stability Constants Database, Academic Software (Version 5.5), R. Soc. Chem., 1993–2005.
6. O. Dömötör, V. F. S. Pape, N. V. May, G. Szakács, É. A. Enyedy, Dalton Trans. 46 2017, 4382–4396. https://doi.org/10.1039/c7dt00439g